https://doi.org/10.5194/egusphere-2026-2195
Preprint. Discussion started: 19 May 2026

Disentangling Mechanistic Controls on Ultrafine Particle Number and Growth Across Seasons in an Urban Street Canyon

Yanxia Li[1], Hengheng Zhang[1,a], Xuefeng Shi[1], Yaowei Li[2,b], Sophie Abou-Rizk[2], Jessica B. Smith[2], Zhaojin An[2,c], Adrian Wenzel[3], Junwei Song[4], Thomas Leisner[1,5], Frank Keutsch[2], Jia Chen[3], and Harald Saathoff[1]

[1]Institute of Meteorology and Climate Research Atmospheric Aerosol Research, Karlsruhe Institute of Technology, 76344 Eggenstein-Leopoldshafen, Germany
[2]Paulson School of Engineering and Applied Sciences, Harvard University, Cambridge, MA 02138, USA
[3]Environmental Sensing and Modeling, Technical University of Munich (TUM), Munich, Germany
[4] School of Marine Sciences, Sun Yat-sen University, Zhuhai 519082, China
[5]Institute of Environmental Physics, Heidelberg University, 69120 Heidelberg, Germany
[a]now at: Research Institute for Applied Mechanics, Kyushu University, Fukuoka, Japan
[b]now at: Department of Earth, Atmospheric, and Planetary Sciences, Massachusetts Institute of Technology, Cambridge, MA 02139, USA
[c]now at: School of Environment, Tsinghua University, 10084, Beijing China

Corresponding authors: Yanxia Li (yanxia.li@kit.edu) and Harald Saathoff (Harald.Saathoff@kit.edu)

Abstract: Ultrafine particles (UFP; <100 nm diameter) play a disproportionate role in human health and atmospheric processes, yet their sources and growth mechanisms in urban environments in different seasons remain poorly constrained. This study presents a comprehensive characterization of UFP number concentrations, size distributions, chemical drivers, and meteorological influences in downtown Munich across summer, winter, and spring. We combine high resolution particle number size measurements with source characterization of organic aerosol (OA), semi-volatile organic aerosol (SVOA) and volatile organic compounds (VOC) to disentangle primary emissions from secondary processes. Results show that UFP number concentrations are driven by traffic- and cooking-related emissions, consistently peaking during nighttime boundary layer collapse due to accumulation. In contrast, ultrafine particle growth (from 40 to 80 nm) arises predominantly from condensation of semi-volatile or low-volatility organic vapours, with distinct seasonal pathways: biogenic and biomass burning OA at night, and photochemically oxidized low-volatility vapours during daytime in summer; biomass-burning and combustion-related SVOA in winter; and a mixed regime involving both primary emissions and moderate photochemistry in spring. No evidence of classical new particle formation appears in these non-nucleation UFP growth events. These findings demonstrate that UFP evolution in Munich is governed by the interplay between boundary-layer dynamics and seasonally varying organic vapour sources, highlighting the need for season-specific mitigation strategies.

1. Introduction

Ultrafine particles (UFP), defined as airborne particles with diameters below 100 nm, have received increasing attention due to their potential to penetrate deeply into the human respiratory tract and translocate into the circulatory system (Zhang et al., 2015; Schraufnagel, 2020; Bousiotis et al., 2021a; Flood-Garibay et al., 2023; Folwarczny et al., 2025). A recent White Paper identified the lack of harmonized measurement protocols and emphasized that UFP composition and sources vary substantially across urban, industrial, and rural environments,

https://doi.org/10.5194/egusphere-2026-2195
Preprint. Discussion started: 19 May 2026

resulting in pronounced spatial and temporal heterogeneity (Morawska et al., 2023; Rattigan et al., 2024; Kecorius et al., 2025). In response, the World Health Organization (WHO) and European Union (EU) have prioritized UFP assessment within its air quality policy framework to better understand their distribution, sources, and health implications across different places (Avl, 2024). The EU has established the EU Air Quality Directive 2024/2881 which, for the first time, requires the monitoring of UFP across the EU as part of national monitoring strategies. However, no limit values have been established so far. The WHO defines UFP number concentrations exceeding 10^4 cm^{-3} (24-hour mean) as high concentrations (Damayanti et al., 2023), a threshold associated with increased health risks including respiratory and cardiovascular effects; however, despite growing regulatory interest, the mechanistic understanding of UFP sources and seasonal growth processes in specific urban environments remains insufficient to inform targeted mitigation strategies.

UFP constitute a major fraction of atmospheric particle number but contribute negligibly to total mass, necessitating particle number concentration (PNC) and size distribution as primary characterization metrics. Urban UFP number concentration and $PM_{2.5}$ mass concentration are poorly correlated (r = 0.09 - 0.64) but strongly correlated with NO and benzene, indicating motor vehicle emissions as the dominant urban source accounting for 50 - 60% of UFP number concentrations at roadside locations (Varotsos et al., 2012; Kumar et al., 2014; De Jesus et al., 2019; Abdillah et al., 2024; Wang et al., 2024). Multiple studies reveal consistent spatial UFP number concentration gradients across urban environments (Giemsa et al., 2021). A Switzerland study across 80 residential sites reported median UFP number concentrations ranging from 6900 - 14700 particles cm^{-3} between urban and rural areas (Meier et al., 2015). Similar spatial patterns have also been observed in other metropolitan regions. A Boston metropolitan study further demonstrated a clear spatial trend: concentrations were highest on-road (32,000 - 64,000 particles cm^{-3}), intermediate at central sites (19,000 - 23,000 particles cm^{-3}), and lowest in residential areas (14,000 - 15,000 particles cm^{-3}), with traffic-related peaks observed during rush hours (Simon et al., 2017). PNC follows traffic > urban > suburban patterns, increasing from Northern/Western to Southern/Eastern Europe. Environmental conditions, particularly temperature (R = 0.814) and relative humidity (R = 0.787), drive nucleation processes alongside traffic emissions as dual urban UFP sources. The sources of UFP vary by site type: at traffic-dominated sites, UFP number concentrations are primarily driven by direct vehicle emissions, as reflected by strong positive correlations between PNC and equivalent black carbon (eBC); whereas in cities with high solar radiation, photochemical particle formation becomes a significant secondary source, evidenced by midday UFP peaks and seasonal anti-correlation between PNC and eBC. Some sites exhibit contributions from both sources (Li et al., 2023a; Trechera et al., 2023). UFP size distributions measured via Scanning Mobility Particle Sizer (SMPS)/Mobility Particle Size Spectrometer (MPSS) reveal distinct patterns across geographic locations and seasons. A Paris urban background study (2019 - 2022) measured mean PNC of 8,100 ± 4,800 particles cm^{-3} (8 - 100 nm), with predominant 20 - 30 nm particles linked to vehicular emissions (Abbou et al., 2024). Nucleation mode particles (< 25 nm) constitute significant proportions due to ineffective Diesel Particle Filters and inadequate semi-volatile organic compound controls, substantially influencing overall UFP trends (Chen et al., 2023; Garcia-Marles et al., 2024a). A 2022 Delhi study found nucleation mode particles (10 -30 nm) contributed ~50% during summer daytime from fresh traffic emissions, with size modes shifting from nucleation and Aitken (30-100 nm) during daytime to Aitken and accumulation modes (100 - 1000 nm) at night (Mohan et al., 2024; Teinilä et al., 2025). In contrast, a Helsinki winter study reported high sub-10 nm particle concentrations across all locations, indicating pronounced seasonal and geographic variations in UFP size distributions (Lepisto

https://doi.org/10.5194/egusphere-2026-2195
Preprint. Discussion started: 19 May 2026

et al., 2023). Nevertheless, most of these studies rely mainly on particle number and size distribution measurements, without sufficient means to distinguish between primary emissions and secondary particle formation and growth.

In recent years, multiple complementary methodologies have enabled comprehensive source identification and composition analysis of UFP. Particle number size distribution (PNSD) measurements via SMPS form the foundation for UFP source identification, revealing that traffic emissions contributed 29 - 39% of particle number while secondary formation accounted for 61-71% (Dall'osto et al., 2013). At Leipzig urban roadside sites, traffic was the dominant primary source (52%), while the remaining contributions arose from secondary or non-local processes: diffuse urban sources (20%), reflecting city-wide oxidation of volatile organics and minor combustion emissions; regional background (21%), representing long-range transport of photochemically aged aerosols; and new particle formation (7%), driven by gas-to-particle conversion of sulfuric acid and organic vapours during low-condensation-sink conditions (Ma and Birmili, 2015). Multiple cities using k-means clustering identified traffic (44 - 65%), nucleation (14 - 19%), and background (7 - 22%) as major UFP sources, with nucleation potentially increasing as traffic emissions decrease due to reduced condensation sinks (Brines et al., 2015; Ahn et al., 2021; Zhao et al., 2021). Positive matrix factorization (PMF) applied to PNSD combined with chemical tracers (eBC, NOx, O_3) successfully partitioned UFP sources into primary traffic (56 - 95% at traffic and urban background sites), photochemical nucleation, and secondary formation processes (Garcia-Marles et al., 2024b; Tao et al., 2023). Quantitative relationships between PNC and source-apportioned eBC enabled traffic, solid fuel burning, and secondary formation contributions to be distinguished across diverse environments (Hama et al., 2017; Xiang et al., 2023). Chemical composition analysis reveals organic components dominate urban UFP (68-81%), with seasonal variations: CHO organics peak in summer while sulfur- and nitrogen-containing organics, nitrate, and chloride dominate winter, with contributions from cooking, vehicle emissions, photooxidation, and aqueous/heterogeneous processes (Li et al., 2023b). Lintusaari et al. (2023) using a volatility condensation particle counter battery (CPCB) with cutoff sizes combined with thermal treatment to identify non-volatile particles, sub-23 nm non-volatile particles were found to dominate traffic emissions, with sub-10 nm particles showing 3 times higher emission factors than larger particles. Hybrid PMF analysis incorporating both size-driven and composition-driven factors revealed that daytime nucleation involved ammonium sulphate and moderately oxygenated organic aerosol, while growth was facilitated by hydrocarbon-like and low-oxygenated organic aerosols and nitrate (Ajith et al., 2024). Mechanistically, traffic-derived organics, sulfuric acid, and amines (especially C_2-amines) drive urban UFP nucleation and growth rather than NO_x levels, with organically-oxygenated molecules critical for particle formation and survival at roadsides despite high condensation sinks (Saarikoski et al., 2023; Guo et al., 2020; Brean et al., 2024; Brean et al., 2025). Additionally, cooking emissions represent a significant UFP source dominated by organic aerosol with reduced-nitrogen species (amine/imide functionalities) comprising 15-50% of organic mass, indicating both traffic and cooking as important anthropogenic UFP precursor sources (Kim et al., 2024). However, few studies have simultaneously integrated gas-phase VOC, particle-phase OA/SVOA source apportionment, and size distribution measurements across multiple seasons in a single urban street canyon. Therefore, leaving the seasonal chemical drivers of UFP growth poorly constrained.

https://doi.org/10.5194/egusphere-2026-2195
Preprint. Discussion started: 19 May 2026

In contrast to previous studies that have primarily relied on particle number size distributions combined with limited chemical tracers such as eBC and NO_x for UFP source apportionment, this investigation uniquely integrates gas- and particle-phase chemical composition measurements. We employed a Condensation Particle Counter (CPC), a Scanning Mobility Particle Sizer (SMPS), a High-Resolution Time-of-Flight Aerosol Mass Spectrometer (HR-TOF-AMS), and a Chemical Analysis of Aerosol Online coupled with Proton Transfer Reaction Mass Spectrometry (CHARON-PTR-MS) to characterize seasonal particle number concentrations, size distributions, new particle formation and growth events in an urban street canyon in Munich, Germany. This approach enables, for the first time in a European street canyon, a distinction between primary emission-driven UFP number concentration peaks and secondary organic vapour condensation-driven UFP growth across three seasons. This is going well beyond explanations reported in the literature focusing on traffic emissions and nucleation. Our measurements elucidate how the seasonal variability of organic vapour sources governs UFP growth, and number concentrations in an urban street canyon environment, ranging from primary traffic and cooking emissions in winter to photochemically oxidized biogenic and biomass-burning compounds in summer.

2. Methods

2.1 Measurement location

Field observations were conducted at the same location in urban Munich (11°57'E, 48°15'N; elevation 520 m a.s.l.) during three seasons: summer (August 3-29, 2023), late winter (March 1-8, 2024), and spring (March 9-27, 2024). The sampling site is located at Theresienstrasse 39 within an urban street canyon adjacent to a 30 m tall building of Ludwig-Maximilians-Universität München (LMU). The surrounding area comprises restaurants, residential buildings, museums, and university workshops and laboratories, with substantial vehicular traffic. Due to the street-canyon configuration and the building-induced flow, wind direction at street level predominantly originates from the south and southeast, reflecting a vortex effect on the lee side of the LMU building where the measurement site is located. In contrast, winds at the rooftop level (30 m) mainly originate from the west and east. More details on the site characteristics during the measurement campaigns are provided in Li et al. (2026).

2.2 Instrumentation

All instruments were placed in the measurement container (Figure S1). A total suspended particle (TSP) inlet was used for sampling of particles and gases, while a $PM_{2.5}$ aerodynamic inlet (16.7 L min^{-1}) was employed to restrict particle sampling to those with aerodynamic diameters below 2.5 µm. The TSP and $PM_{2.5}$ inlets were mounted on the roof of the measurement container and connected to the instruments inside via stainless steel sampling lines of 2 m and 1.5 m, respectively. The TSP inlet supplied sample air to the CPC, U-SMPS, and FIDAS 200. The $PM_{2.5}$ inlet split at its downstream end into three separate lines: the HR-TOF-AMS inlet was located 0.5 m from the splitting point via a stainless-steel line, the CHARON-PTR-MS inlet was located 1 m away via a stainless-steel line, and the fiber laser-induced fluorescence (FILIF) inlet was connected via a 1 m PFA line following a stainless-steel-to-PFA connector at the splitting point. Gas-phase measurements (O_3, NO_2, NH_3, and VOCs via PTR-MS) were conducted through a dedicated 2 m PFA line mounted alongside the TSP inlet. A schematic of the sampling setup is provided in Figure S1. Particle number concentrations were measured using condensation particle counters (CPC): a CPC 3776 (TSI Inc.) detecting particles >2.5 nm throughout the study period with 1 s

https://doi.org/10.5194/egusphere-2026-2195
Preprint. Discussion started: 19 May 2026

time resolution, a CPC 3756 (TSI Inc.) for particles >2.5 nm in August 2023 (1 s resolution), and a CPC 3022 (TSI Inc.) for particles >7 nm in March 2024 (1 s resolution). Particle size distributions were measured using two different systems: a Universal Scanning Mobility Particle Sizer (U-SMPS 2050, Palas GmbH) covering 7-763.5 nm (4 min time resolution, August 2023) and an SMPS (DMA 3081, TSI Inc.) covering 14-763.5 nm (6 min time resolution, March 2024). Mass concentrations of PM_1, $PM_{2.5}$, PM_4 and PM_{10} were calculated based on size distributions measured using a FIDAS 200 (Palas GmbH) with 1 s time resolution. Equivalent black carbon (eBC) was measured by an AE33 (Magee Scientific) with 1 min resolution. Meteorological parameters (WS700, Lufft GmbH) were recorded at 1 s resolution. Trace gases were monitored at 1 min time resolution: NO_2 (AS32M, Environment SA) and O_3 (O341M, Environment SA), while NH_3 (G2103, Picarro) was measured at 2 min resolution. Volatile organic compounds (VOCs) in the gas phase and semi-volatile organic compounds in the particle phase were measured using a proton-transfer-reaction time-of-flight mass spectrometer (PTR-TOF-MS 4000X2, Ionicon Analytik GmbH) equipped with a particle inlet (Chemical Analysis of aeRosol ONline, CHARON), with 10 s time resolution. Non-refractory $PM_{2.5}$ (NR-$PM_{2.5}$) components were quantified using a high-resolution time-of-flight aerosol mass spectrometer (HR-TOF-AMS, Aerodyne Research Inc.) equipped with a $PM_{2.5}$ aerodynamic lens at 1 min time resolution. The HR-TOF-AMS provides reliable chemical composition measurements for particles in the 70 - 600 nm size range, and therefore the composition data reported here primarily reflect the larger UFP fraction, with limited sensitivity to sub-60 nm particles (Aktypis et al., 2024). Similarly, the CHARON-PTR-MS detects particles in the 60 - 600 nm size range, but shows reduced particle enrichment efficiency for particles in the 60 - 150 nm size range, meaning that the semi-volatile organic composition data reported here are most representative of particles larger than 150 nm (Muller et al., 2017). However, source factors derived from larger particles can be correlated with UFP size evolution, and gas-phase VOC source factors from PTR-MS provide additional constraints on UFP formation and growth processes across all size ranges. Therefore, while the chemical composition data should be interpreted with these size-dependent limitations in mind, the combined OA/SVOA and VOC source apportionment approach adopted here remains valid for identifying the dominant chemical drivers of UFP dynamics. Formaldehyde was detected using FILIF with ± 27 pptv precision at 10 Hz sampling frequency. CHARON-PTR-MS raw data were processed using IONICON Data Analyzer software (IDA 2.2.0) following established protocols, while AMS data were processed using SQUIRREL 1.65G and PIKA 1.25G. VOC and SVOA from CHARON-PTR-MS were analysed using SoFi Pro 9.0 for exploratory factor analysis, while organic aerosols from AMS underwent source apportionment via PMF Evaluation Tool (v3.08C) in IGOR Pro (v8.04). More details on the instrumentation during the measurement campaigns are provided in Li et al. (2026).

To investigate the influence of air mass origins on atmospheric pollutants, 72 - hour backward trajectories arriving at the measurement site at an altitude of 500 m a.g.l. were computed hourly using MeteoInfoMap (Wang, 2019), an open-source trajectory tool referenced on the Hybrid Single-Particle Lagrangian Integrated Trajectory (HYSPLIT) model website (Cohen et al., 2015), driven by Global Data Assimilation System (GDAS) meteorological fields.

https://doi.org/10.5194/egusphere-2026-2195
Preprint. Discussion started: 19 May 2026

3. Results and Discussion

3.1 Overview of Ultrafine Particles in Munich

In this section the ultrafine particle number concentrations as well as the variations of particle size distributions during the different seasons will be discussed.

3.1.1 Seasonal Variations in Particle Number Size Distributions

The Particle Number Size Distributions (PNSD) of ultrafine aerosols in the Munich urban area exhibit pronounced seasonal variability, strongly correlated with ambient temperature and atmospheric processes. Similar seasonal variability in ultrafine particle size distributions has also been reported in other urban environments, particularly in European cities such as Helsinki and Leipzig, where particle number concentrations are strongly influenced by temperature-dependent photochemistry and boundary-layer dynamics (Ma and Birmili, 2015; Rose et al., 2021). High average summer temperatures (21.9 ± 5.8 °C) promoted the dominance of the organic aerosol fraction (Org) (Figure 1d, h) and facilitated UFP growth events, particularly during nocturnal periods (Figure 1c, g). These nighttime UFP growth events are likely driven by the condensational growth of semi-volatile organic compounds (SVOCs) onto the particle phase provided by traffic primary particles. Li et al. (2023b) also identified oxidized organic species as dominant contributors to nighttime UFP growth in urban Beijing, suggesting that condensation of secondary organic vapours onto primary traffic particles is a common nocturnal growth mechanism across diverse urban environments. Conversely, the significantly colder winter/spring period (8.4 ± 3.0 °C / 10.2 ± 3.8 °C) presented a more dynamic composition: nitrate dominated in early March (1st - 8th) due to its stability at lower temperatures, before shifting to organic dominance later in that month (9th - 27th) as solar radiation and temperature increased. The nitrate-dominated winter composition observed in Munich aligns with observations in northern France and Helsinki, were low temperatures favour nitrate partitioning onto larger particles, suppressing UFP formation (Roig Rodelas et al., 2019; Lepisto et al., 2023). This seasonal change is also reflected in the UFP number concentration fraction, which was significantly lower in winter (70.4 ± 9.2%) compared to summer and spring (82.0 ± 7.9% and 82.0 ± 6.7%, respectively), potentially due to a lower frequency of new particle formation and enhanced condensational sink during the colder season. Rose et al. (2021) reported higher UFP fractions during warmer months across multiple GAW network sites, attributing this pattern to enhanced photochemical nucleation and growth.

https://doi.org/10.5194/egusphere-2026-2195
Preprint. Discussion started: 19 May 2026

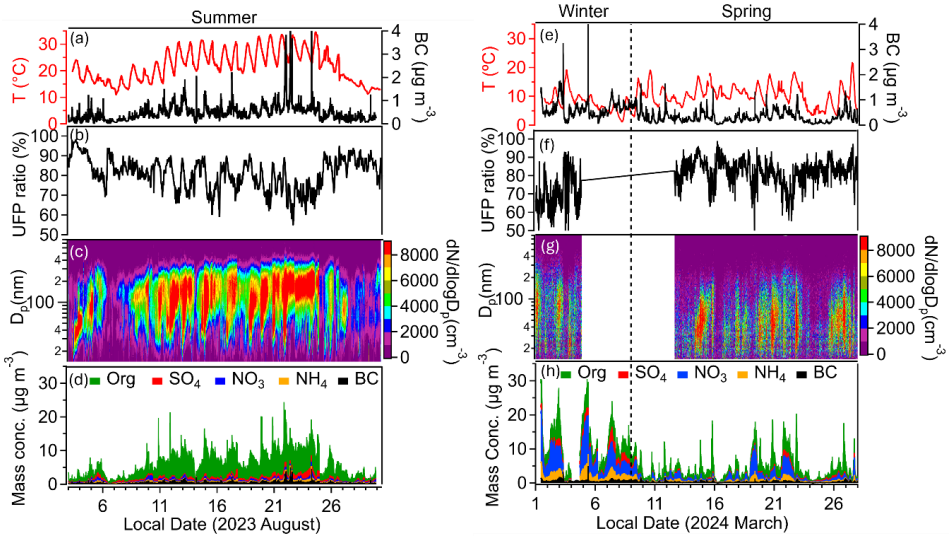

Figure 1. Seasonal characteristics of temperature (T) and equivalent black carbon (eBC) concentrations (a,e); UFP number concentration (Percentage of D_p<100 nm compared to total particle number concentration) (b,f); time-resolved particle number size distributions ($dN/dlogD_p$) (c, g); and mass concentrations of major non-refractory aerosol species measured by the AMS (organic aerosol, sulfate, nitrate, ammonium) along with eBC (d, h) measured in Munich during summer (August 2023) and winter–spring (March 2024).

3.1.2 Seasonal Variations in UFP Number Concentrations

The pronounced and size-dependent seasonal variability in ultrafine PNC in the Munich urban area, are reflecting distinct atmospheric production and removal mechanisms across seasons. Focusing first on the smaller size fraction (14 nm < D_p < 25 nm), which captures recently formed particles in the nucleation and lower Aitken mode and is most sensitive to new particle formation (NPF) events. The highest median and mean concentrations are recorded in summer, accompanied by the widest variability (Figure 2a). This pattern strongly suggests that summer is characterized by frequent and rapid UFP growth events, driven by enhanced night-time oxidation and photochemical activities (higher OH, O_3), elevated biogenic volatile organic compound (BVOC) emissions, and favourable meteorological conditions that promote UFP growth (Sun et al., 2024). Winter registers the lowest concentrations, approximately half the summer values, indicating fewer dynamic atmospheric processes. This is attributed to suppressed photochemistry, reduced BVOC emissions, and potentially a stable boundary layer that limits nucleation. Stable boundary layers suppress atmospheric new particle formation (NPF) by reducing turbulent mixing and precursor transport, while simultaneously increasing the condensation sink as primary emissions accumulate near the surface, thereby favouring condensation onto pre-existing particles over new particle nucleation (Hao et al., 2018; Carrillo-Cardenas et al., 2025).

The seasonality in the UFP numbers is significantly attenuated in the size range (25 nm < Dp < 100 nm), suggesting that these particles are influenced more by growth processes and primary emissions than by nucleation bursts (Figure 2b). Unlike the nucleation mode fraction (14 nm < D_p < 25 nm) discussed above, they show much smaller differences across seasons compared to the nucleation mode particles, with variability remaining consistent (Rose et al., 2021). Notably, winter concentrations in this size range are slightly elevated relative to the other seasons, in contrast to the nucleation mode where summer dominates. This suggests a potential influence

https://doi.org/10.5194/egusphere-2026-2195
Preprint. Discussion started: 19 May 2026

from stable primary combustion sources (e.g., traffic and heating) which contribute consistently to this size bin (Okuljar et al., 2021; Sun et al., 2024).

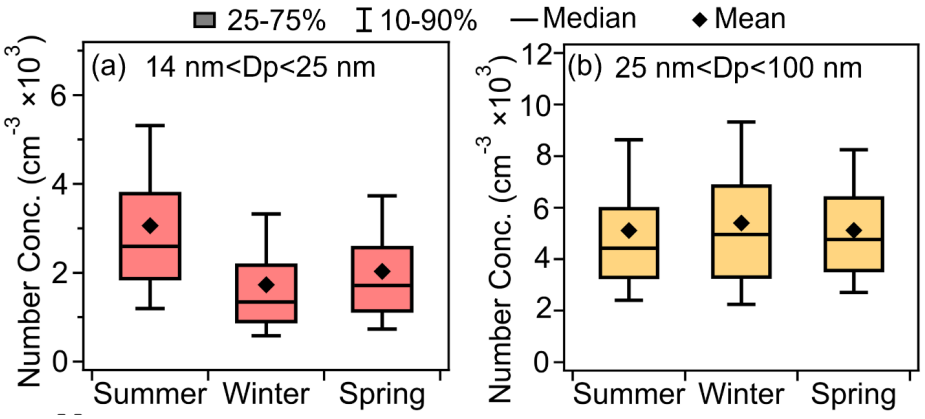

Figure 2. Seasonal variations of particle number concentrations for (a) 14-25 nm and (b) 25-100 nm diameter size ranges in summer, winter, and spring. Box plots show the median, mean, 25-75th percentiles, and 10-90th percentiles. *Please note that winter UFP data were limited to three days (1st - 3rd March) due to a power outage, and the following seasonal comparisons should be interpreted with this limitation in mind.

3.1.3 Diurnal variation of particle size distributions in different seasons

Seasonal differences in particle size distributions in Munich reflect the influence of particle composition on ultrafine particle behaviour. Figure 3 illustrates that the smaller particles (14nm < D_p < 25nm) show the most drastic change, with PNC in summer being significantly higher than in spring and winter. This is attributed to the dominance of secondary photochemical processes at high summer temperatures and intense solar radiation (Birmili et al., 2010). The summer aerosol mass is dominated by the organic fraction (Org), which exhibits a strong late-evening peak (21:00 - 22:00) accompanied by shrinking planetary boundary layer (PBL) heights (Figures 4, 5 and 6) and the enhanced condensation of semi-volatile organic compounds (SVOCs) like oxidized biogenic compounds (Li et al., 2017; Liaskoni et al., 2024). This high concentration of low-volatility organic material drives the observed UFP growth events (Haeffelin et al., 2024), particularly those occurring nocturnally, efficiently growing particles into the Aitken mode. Conversely, the significantly colder winter/spring period suppresses photochemical production and shows much lower UFP ratios due to a combination of reduced NPF and increased condensational sink by pre-existing particles (Rose et al., 2021). Furthermore, the cold season shifts the chemical regime: Nitrate dominates in winter, particularly in early March, due to its stability in the particle phase at lower temperatures (Roig Rodelas et al., 2019). Since nitrate primarily condenses onto larger particles, it inhibits NPF and UFP growth, resulting in a noisy PNSD lacking a clear nucleation signal. Spring is a transitional period, where the midday nucleation mode partially recovers alongside an evening increase in organic aerosol, indicating the revival of photochemical activity; however, remaining nitrate-rich particles enhance the condensation sink and favour the partitioning of condensable vapours onto larger particles (Roig Rodelas et al., 2019; Lepisto et al., 2023), which limits the growth efficiency of newly formed ultrafine particles compared with summer. These seasonal differences are also reflected in the diurnal variations of the geometric mean diameter (GMD) shown in Fig. 3(g). The mean GMD values are consistently larger than 30 nm across all seasons. The smallest GMD values occur in summer, indicating a higher abundance of smaller particles associated with active

https://doi.org/10.5194/egusphere-2026-2195
Preprint. Discussion started: 19 May 2026

264 particle formation and growth processes. In contrast, winter exhibits the largest GMD values, reflecting the
265 stronger influence of aged and larger particles under conditions of suppressed photochemical activity. Spring
266 shows intermediate behaviour, consistent with its transitional atmospheric conditions.

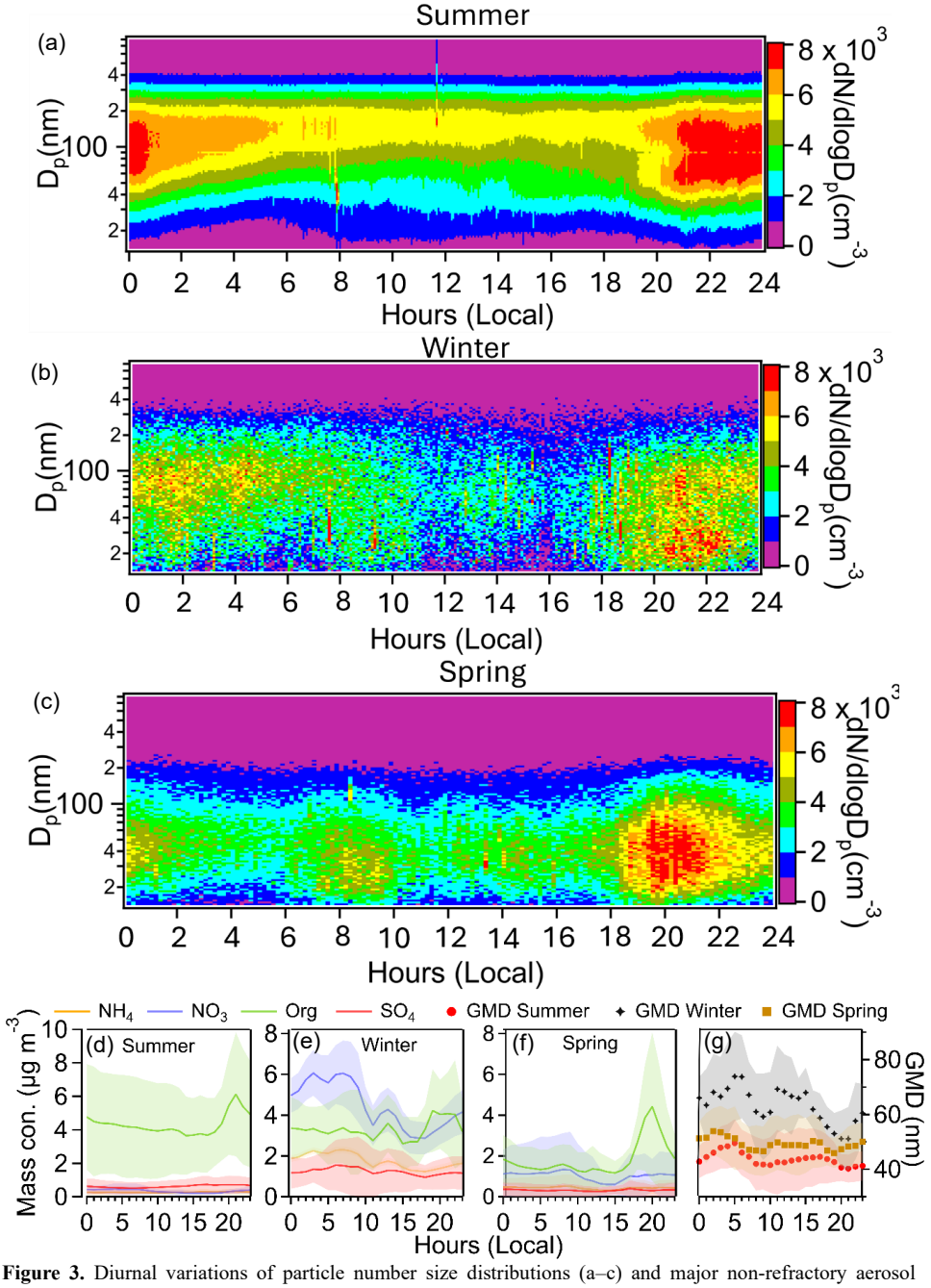

Figure 3. Diurnal variations of particle number size distributions (a–c) and major non-refractory aerosol components measured by the HR-ToF-AMS (organic aerosol, nitrate, ammonium, and sulfate) (d–f) during

https://doi.org/10.5194/egusphere-2026-2195
Preprint. Discussion started: 19 May 2026

summer, winter, and spring. Lines show the diurnal mean values, and shaded areas represent the seasonal variability. Panel (g) shows the diurnal variations of particle geometric mean diameter (GMD).

3.2 Seasonality of chemical drivers of ultrafine particle growth

To illustrate the chemical drivers of seasonal UFP growth in detail, we focus on representative 48-hour observation windows selected from each season of the two measurement campaigns (summer 2023 and winter/spring 2024). These periods were chosen because they capture multiple recurring growth events with consistent temporal patterns, including nighttime number concentration peaks followed by gradual size increases, that are representative of the broader seasonal behaviour documented in the full dataset. Similar growth sequences were observed repeatedly throughout each season, confirming that the selected periods are not isolated anomalies but reflect systematic and recurring atmospheric processes.

Investigating the chemical factors governing seasonal UFP growth, Figure 4 provides a detailed characterization of representative UFP growth events, defined here as increases in geometric mean diameter (GMD) without concurrent new particle formation or sub-25 nm particle bursts, by linking UFP dynamics with organic aerosol (OA) source factors derived through PMF, organic mass, boundary layer height (BLH), and particle size distributions in summer. The data collectively demonstrate that the summer UFP population is fundamentally regulated by an interplay between primary emissions and subsequent secondary organic vapor condensation. These UFP growth events occurred frequently at night, particularly between 00:00 and 04:00, during which the geometric mean diameter (GMD) particle sizes increased from about 40 nm to 60 nm. Importantly, each growth event was preceded by strong particle number peaks associated with evening traffic emissions and shrinking BLH, which trapped primary particles from traffic and cooking within the shallow nocturnal boundary layer. The strong correlations between UFP concentrations and traffic- and cooking-related OA (R = 0.74 and 0.49, respectively; Table S1), together with the significant correlation with traffic VOCs (R = 0.55; Table S1), confirm the dominant role of primary emissions during these pre-growth periods. After these sources stabilized or declined, particle growth proceeded. Source apportionment indicates that the subsequent size increase was driven by the condensation and coagulation of semi-volatile and low-volatility organics, particularly biogenic organic aerosol (BOA) and biomass burning organic aerosol (BBOA), while cooking OA became negligible. This interpretation is supported by Figure 4, which shows nighttime peaks in LV-OOA, BOA, and BBOA coincident with UFP growth, and by Figure S3, which illustrates concurrent increases in BBOA, isoprene-oxidized OA & BBOA, regional background OA, weakly oxidized BOA, more oxidized BOA, and black carbon. New particle formation played little or no role, as OA concentrations and precursor VOCs generally peaked before growth initiation. A distinct midday growth event was also observed, characterized by strong increases in BBOA, low volatile oxygenated organic aerosol (LV-OOA), and black carbon while other primary sources and total particle numbers remained low, indicating that photochemical oxidation of biomass-burning and low-volatility organic vapors dominated this daytime growth. Consistent with this interpretation, Figure S2 shows midday increases in biomass-burning and aged VOCs, and Figure S3 shows corresponding peaks in BBOA and isoprene-oxidized OA & BBOA. Early-morning growth is supported by several secondary OA components except cooking OA, whereas midday growth is predominantly linked to photochemically oxidized biomass-burning emissions.

https://doi.org/10.5194/egusphere-2026-2195
Preprint. Discussion started: 19 May 2026

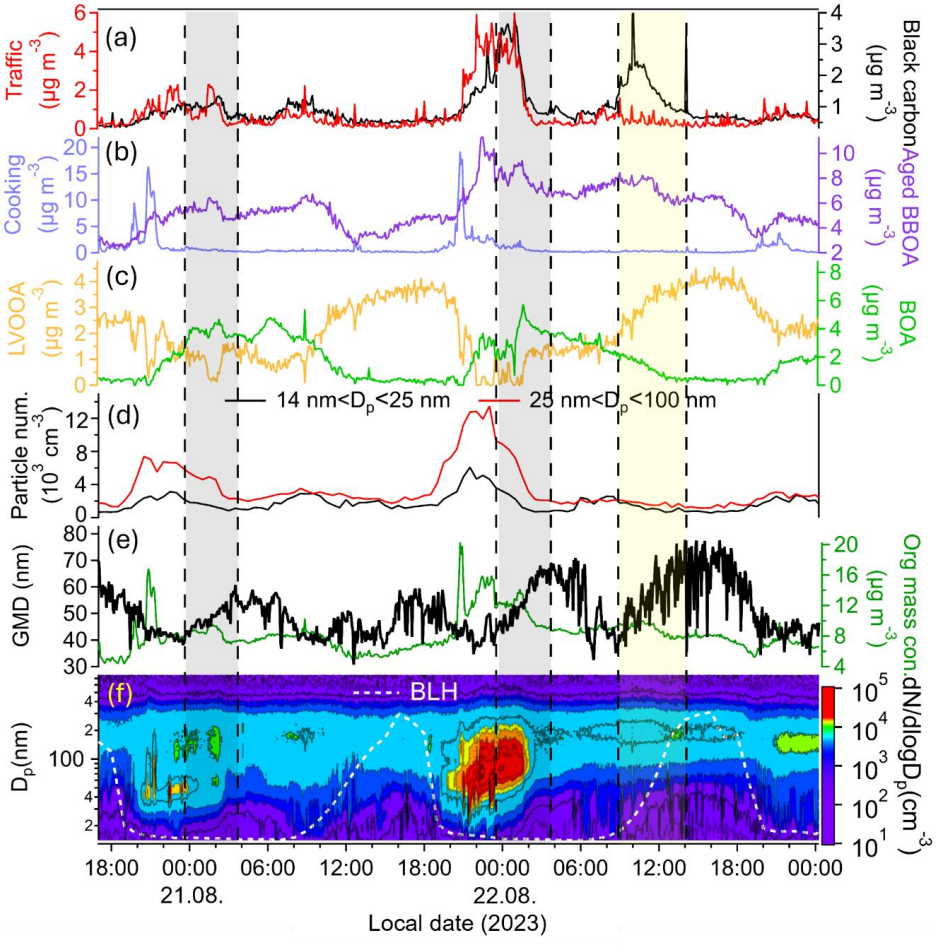

Figure 4. Representative evolution of organic aerosol source factors derived through AMS-PMF and UFP size distribution properties during the summer period. Panels show (a) Traffic OA and black carbon, (b) Cooking OA and Aged BBOA, (c) major secondary OA components (LVOOA, BOA), (d) number concentrations of 14-25 nm and 25-100 nm particles, (e) geometric mean diameter (GMD) and total organic mass concentration, and (f) particle number size distribution ($dN/dlogD_p$) with boundary layer height (BLH). Grey shaded regions denote night time non-nucleation UFP growth periods; the yellow shaded region denotes daytime UFP growth periods.

Winter UFP behaviour shows a similar temporal pattern compared to summer in terms of peak number concentrations, with UFP number concentration increases occurring almost exclusively during nighttime and early morning when the BLH decreases and remains very shallow, allowing primary emissions to accumulate near the surface. However, the chemical drivers differ substantially from those in summer. Due to a power outage, winter UFP data were only available for 1st - 3rd March. Although this limits the generalisability of the winter results, these observations suggest that UFP growth during this period is primarily governed by primary combustion emissions and the trapping of semi-volatile species within a shallow boundary layer, rather than photochemical SOA formation. This pattern is broadly consistent with wintertime UFP behaviour reported in comparable European urban environments (Roig Rodelas et al., 2019; Lepisto et al., 2023). Strong correlations between UFP

https://doi.org/10.5194/egusphere-2026-2195
Preprint. Discussion started: 19 May 2026

concentrations and organic aerosol from traffic (R = 0.75) and cooking (R = 0.69) (Table S2) confirm that primary anthropogenic emissions dominate the initial number concentration peaks (Figure 5). In addition, SVOA factors, especially nighttime-aged BBOA, which shows the highest correlation with UFP (R = 0.86), exhibits temporal behaviour closely aligned with UFP growth periods (Fig. S5), indicating that condensation of semi-volatile biomass-burning emissions strongly enhances wintertime particle growth. UFP growth from ~40 nm to ~80 nm occurs during periods of elevated SVOA concentrations, particularly nighttime-aged (R = 0.86) and daytime-aged BBOA (R = 0.53), regional background SVOA (R = 0.79), and cooking-related organics (R = 0.61). These components rise during the same intervals in which the mean particle size (GMD) increases, while total particle number remains steady or declines, consistent with condensation-driven growth and mild coagulation, rather than new particle formation. VOC factor behaviour further supports this primary-emission-driven mechanism: traffic related VOC correlate positively with UFP (Traffic 1: R = 0.47), and background VOC show even stronger associations (R = 0.73), reflecting the accumulation of semi-volatile vapours in a stable nocturnal boundary layer (Fig. S4). Overall, the winter results show that UFP dynamics are governed by primary sources (traffic, cooking, biomass burning) and secondary processing of semi-volatile organics at lower temperatures. Shallow boundary layer hights (BLH) amplify these effects by promoting accumulation and enhancing vapor condensation onto existing particles.

https://doi.org/10.5194/egusphere-2026-2195
Preprint. Discussion started: 19 May 2026

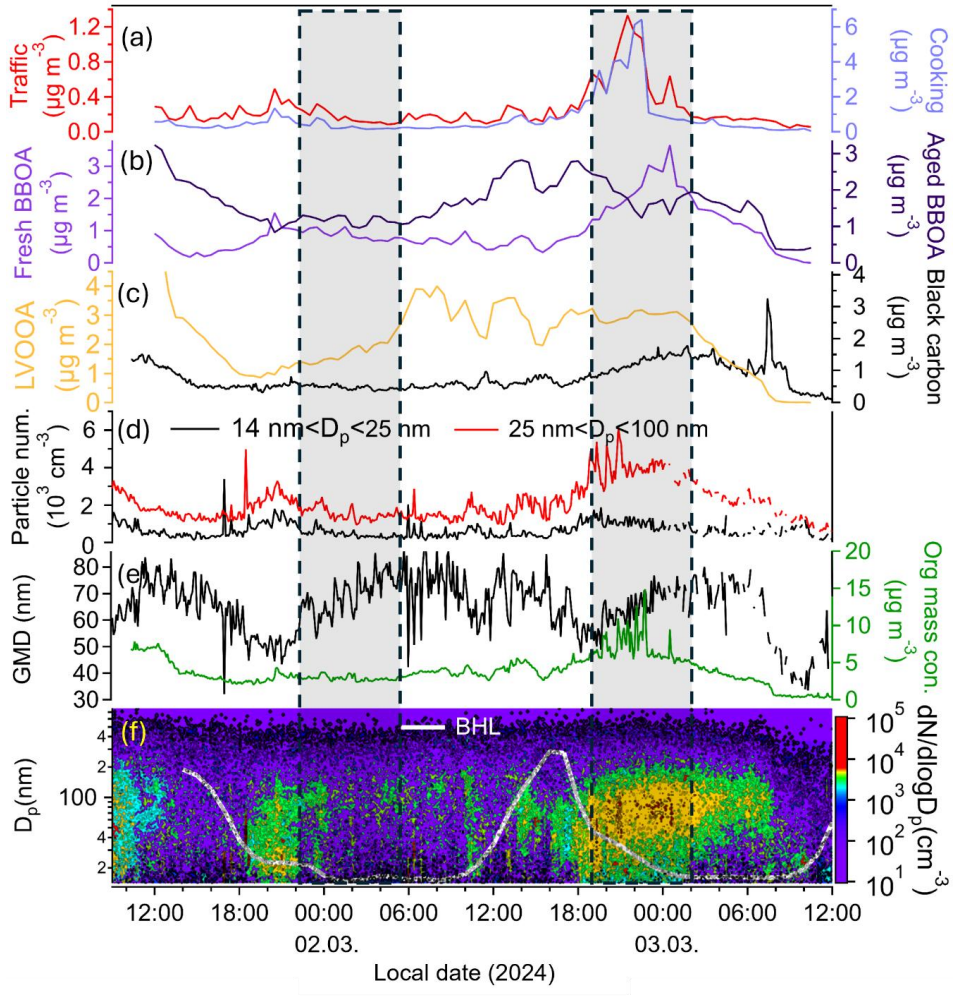

Figure 5. The evolution of organic aerosol source factors and UFP size distribution properties during the winter period (1st – 3rd March). Panels show (a) Traffic and Cooking OA, (b) Fresh BBOA and Aged BBOA, (c) LVOOA and Black carbon, (d) number concentrations of 14-25 nm and 25-100 nm particles, (e) geometric mean diameter (GMD) and total organic mass concentration, and (f) particle number size distribution ($dN/dlogD_p$) with boundary layer height (BLH). Grey shaded regions denote night time non-nucleation UFP growth periods.

Spring UFP behaviour again shows pronounced nighttime and early-morning increases with decreasing and shallow boundary layer hights (BLH), but with a more complex mixture of primary and secondary sources compared to winter. During 9th -27th March, 2024, representative non-nucleation growth events (Fig. 6) reveal that UFP number peaks occur when traffic and cooking emissions accumulate in a shallow boundary layer, followed by periods of particle growth from ~ 40 nm to ~70 - 80 nm. Strong correlations between UFP concentrations and organic aerosol from traffic and cooking (R = 0.74 and 0.70, respectively; Table S3) confirm the dominant role of primary anthropogenic sources in setting the initial number concentration levels. At the same

https://doi.org/10.5194/egusphere-2026-2195
Preprint. Discussion started: 19 May 2026

time, fresh and aged BBOA also correlates relatively well with UFP ($R \approx 0.64$ - 0.66; Table S3), and their time series in Fig. 6 and Fig. S7 show clear enhancements during both night-time and daytime UFP growth periods, indicating that biomass-burning emissions provide an important reservoir of semi-volatile compounds for subsequent condensation. SVOA factors, particularly night-time-aged BBOA ($R = 0.59$), combustion OA and regional SVOA (Fig. S7), rise concurrently with increases in mean particle size (GMD) while total particle number remains nearly constant or decreases, which is consistent with condensation-driven growth and some coagulation rather than new particle formation. The behaviour of VOC source factors further supports this interpretation: Traffic 1 and Traffic 2 VOC (Fig. S6) exhibit strong positive correlations with UFP ($R = 0.73$ and 0.75), while monoterpenes and biomass-burning VOC show weaker correlations ($R \approx 0.4$ and 0.36; Table S3). In contrast, LVOOA shows almost no correlation with UFP, implying that highly aged regional SOA plays only a minor role in the short-term growth episodes observed here. Overall, the spring results indicate that UFP dynamics are controlled by a combination of traffic and cooking emissions, biomass-burning OA and their semi-volatile vapours, with an emerging contribution from photochemically oxidized VOCs.

https://doi.org/10.5194/egusphere-2026-2195
Preprint. Discussion started: 19 May 2026

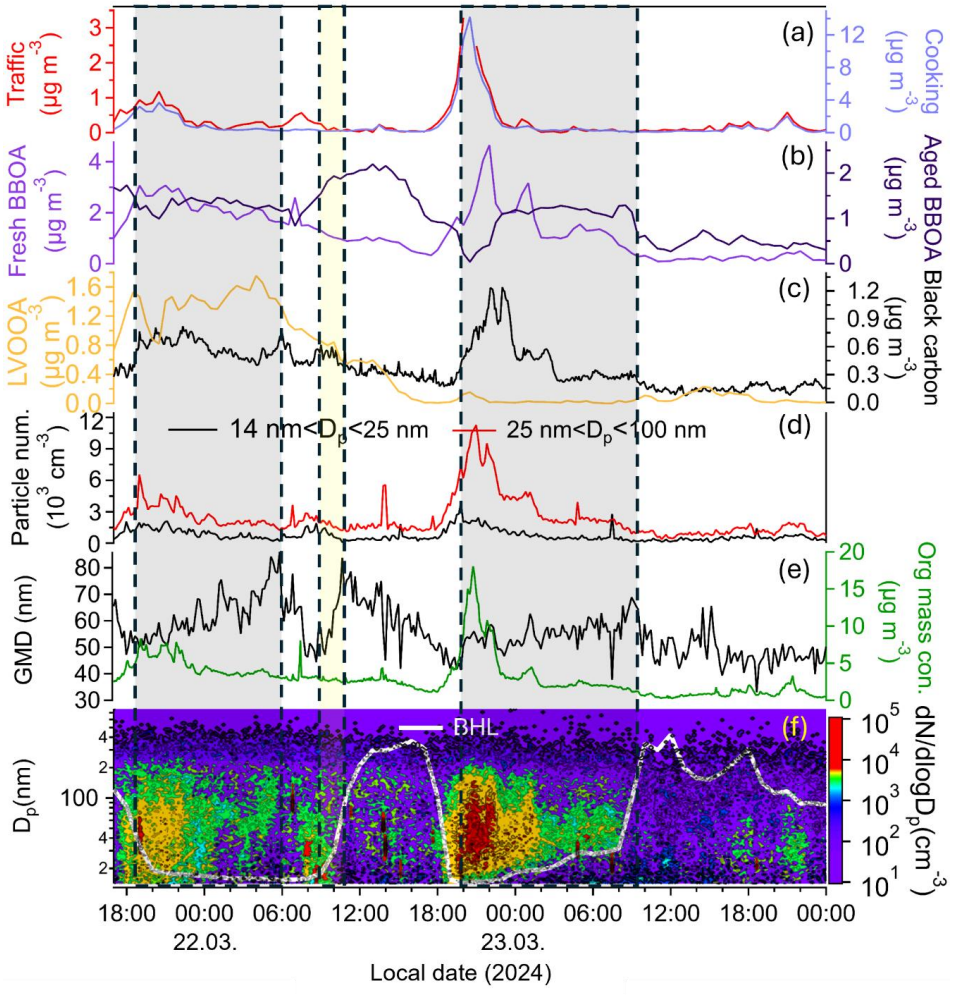

Figure 6. Representative evolution of organic aerosol source factors and UFP size distribution properties during the spring period. Panels show (a) Traffic OA and Cooking OA, (b) Fresh BBOA and Aged BBOA, (c) LVOOA and Black carbon, (d) number concentrations of 14 - 25 nm and 25 - 100 nm particles, (e) geometric mean diameter (GMD) and total organic mass concentration, and (f) particle number size distribution ($dN/dlogD_p$) with boundary layer height (BLH). Grey shaded regions denote night time non-nucleation UFP growth periods; the yellow shaded region denotes a daytime UFP growth period.

Across summer, winter, and spring, UFP number concentrations consistently peaked during nighttime and early morning when the BLH decreased or remained shallow. This similarity highlights the universal importance of BLH-driven accumulation of primary emissions, mainly traffic and cooking, in setting the initial UFP number levels. In all seasons, UFP growth occurred mainly without new particle formation: increases in geometric mean diameter were accompanied by stable or decreasing particle numbers, indicating that growth proceeded through condensation onto pre-existing particles or coagulation at high particle numbers.

https://doi.org/10.5194/egusphere-2026-2195
Preprint. Discussion started: 19 May 2026

Despite these common features, the chemical drivers of UFP growth differed markedly among seasons. In summer, UFP evolution was strongly influenced by secondary organic aerosol formation. Low-volatility oxygenated OA, biogenic OA, and biomass-burning OA increased during growth periods, and daytime growth was linked to photochemical oxidation of biomass burning organic aerosol. In winter, UFP number and growth are governed primarily by traffic, cooking, and biomass-burning emissions. Strong correlations with nighttime-aged BBOA and other semi-volatile OA components indicate that growth was dominated by condensation of semi-volatile vapours at lower temperatures, with minimal photochemical contribution. In spring, UFP behaviour reflected a transitional regime. Nighttime growth resembled winter, driven by primary emissions and biomass-burning SVOA, while emerging photochemical activity supported daytime growth associated with oxidized VOCs and semi-volatile organics. Overall, while BLH-driven accumulation controls UFP number peaks in all seasons, the dominant growth mechanisms shift from photochemical SOA in summer to semi-volatile primary and biomass-burning organics in winter, with spring exhibiting mixed characteristics.

3.3 Atmospheric drivers of seasonal UFP variability

Besides dynamics of emissions, chemical processes, and the urban boundary layer which have been discussed above additional potential drivers of UFP like air mass origin and urban meteorology will be addressed in the following.

3.3.1 Influence of Air Mass Origin

Across the three seasons, clear differences emerge in how regional air mass origins shape UFP size distributions. In summer, four dominant air mass clusters could be identified, including local (C_1), continental (C_2, C_4), and maritime (C_3) air masses as shown in Figure 7 (a-c). Maritime air masses typically transport relatively clean background air with low condensation sinks, favouring both local photochemical formation of ultrafine particles during daytime and nocturnal condensation-driven UFP growth, as the reduced aerosol loading allows semi-volatile organic vapours to partition more efficiently onto pre-existing particles (Salimi et al., 2017; Bousiotis et al., 2021b). In contrast, continental air masses carry more aged regional aerosols with higher condensation sinks, suppressing new particle formation while enhancing accumulation-mode particle fractions (Andreae et al., 2022). In winter, five air mass clusters appear, with strong contributions from northwest and central European pathways (C_1, C_2). These air masses are generally aged and relatively polluted, consistent with the dominance of accumulation-mode particles and limited presence of freshly formed ultrafine particles, reflecting weaker winter photochemistry. Spring exhibits a transitional pattern, with a pronounced contrast between clean maritime inflow (C_3), which supports higher proportions of < 25 nm particles, and continental clusters (C_4, C_5), which transport aged or biomass-burning-influenced aerosols and thus suppress the smallest size fractions. This seasonal contrast is also reflected in the prevailing air mass directions: during summer and spring, air masses are predominantly transported from the westerly marine sector, bringing relatively clean air to Munich, whereas in winter air masses more frequently originate from the easterly continental sector, transporting more polluted and aged aerosols from inland Europe. As a result, summer and spring generally exhibit lower condensation sinks and more favourable conditions for ultrafine particle formation and growth, whereas winter conditions tend to suppress the smallest particle fractions (Giemsa et al., 2021; Hirshorn et al., 2022).

Seasonal wind patterns further reinforce these behaviours: summer winds are stronger and more variable, enhancing dispersion; winter winds are calmer and more stagnant, promoting accumulation of primary UFP; and

https://doi.org/10.5194/egusphere-2026-2195
Preprint. Discussion started: 19 May 2026

spring winds exhibit intermediate characteristics, with episodic easterly flow bringing polluted continental air in as shown in Figure 7(d-f). These meteorological conditions regulate dilution, residence time, and the background concentrations of ultrafine particles available for subsequent growth. Consistent with these patterns, the size-resolved particle number fractions show that, across all clusters, summer exhibits the highest fractions of 14-25 nm particles, while winter shows the lowest, reflecting the suppression of new ultrafine particles under cold and stagnant conditions. Similarly, the combined 14-100 nm particle fraction is smallest in winter, whereas summer and spring both maintain high ultrafine particle fractions (~80%) as shown in Figure 7(g-i), indicating more active photochemical or semi-volatile condensation processes during these seasons.

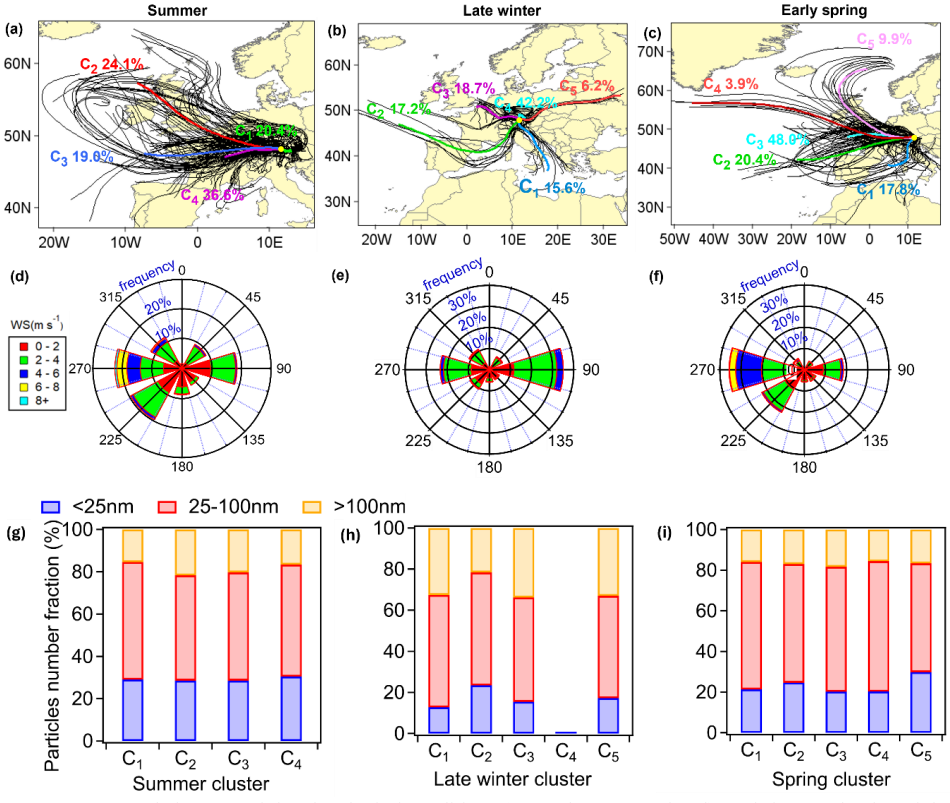

Figure 7. Seasonal air mass origins, local wind conditions (30 m above street level), and size-resolved particle number fractions for summer, late winter, and early spring. Panels (a-c) show 72-h back-trajectory air mass clusters, illustrating distinct source regions and transport pathways for each season (Wang, 2019). Panels (d–f) display wind roses of wind speed and direction measured at 30 m above street level during the respective periods, indicating seasonal differences in prevailing winds and dispersion conditions. Panels (g–i) present the fraction of particle numbers in three size ranges (14–25 nm, 25–100 nm, and 100–800 nm) for each trajectory cluster (no cluster 4 in winter due to limited SMPS data).

3.3.2 Effects of local meteorology on seasonal UFP growth

During two nighttime growth events in summer, Figure 8 shows conditions of lower temperature, high relative humidity, and the absence of solar radiation, under which NO_2-rich traffic-related emissions accumulate. These conditions lead to elevated UFP number concentrations and correspond to traffic- and cooking-dominated periods

https://doi.org/10.5194/egusphere-2026-2195
Preprint. Discussion started: 19 May 2026

(see Figure 4). Following these pre-growth peaks in UFP number concentrations from primary emission, the mean particle size (GMD) increases while particle number declines, indicating particle growth through condensation and coagulation processes. Figure 4 shows that this size growth corresponds to enhanced contributions from LV-OOA, BOA and BBOA, confirming that condensation of semi-volatile and low-volatility organic vapours drives nighttime growth. These conditions favour the accumulation of traffic-related emissions and condensable vapours within the shallow nocturnal boundary layer. During the growth periods, particulate nitrate concentrations remain relatively stable and do not show a concurrent increase, indicating that condensation of inorganic nitrate is unlikely to be the dominant driver of the observed particle growth. Although NH_3 concentrations increase during the preceding emission peaks (Figure 8e), they do not show a clear relationship with the particle growth phase itself, suggesting that NH_3-driven inorganic growth processes likely play only a minor role. The relatively steady levels of formaldehyde and organic aerosol mass further suggest that growth is supported by condensable organic vapours already present in the air mass. However, additional nighttime production of low-volatility vapours through oxidation processes, such as NO_3 radical chemistry, cannot be excluded. Such nighttime particle growth driven by condensation of semi-volatile organic vapours under traffic-influenced urban conditions has been reported in several European field studies (Man et al., 2015; Carnerero et al., 2018). Similar growth behaviour, characterised by increasing GMD following primary emission peaks and decreasing particle number concentrations due to condensation and coagulation, has also been observed in traffic-influenced urban environments (Straaten et al., 2022).

For the daytime growth event, Figure 8 shows relatively high solar radiation, elevated O_3 and reduced NO_2, indicating active photochemistry and somewhat weaker traffic influence. Although formaldehyde and organic mass do not spike sharply, mean particle size (GMD) increases while the 25 - 100 nm mode strengthens, mirroring the particle size evolution shown in Figure 4. The chemical factors shown in Figure 4, especially LV-OOA, BBOA and oxidized VOC-derived SOA can explain this growth, indicating that daytime oxidation processes supply enough low-volatile compounds for efficient condensation even when gas-phase precursor signals vary smoothly. Across European sites, daytime photochemistry supplies oxidized VOCs for growth despite variable emissions, boundary-layer dilution controlling particle number concentrations (Carnerero et al., 2018).

https://doi.org/10.5194/egusphere-2026-2195
Preprint. Discussion started: 19 May 2026

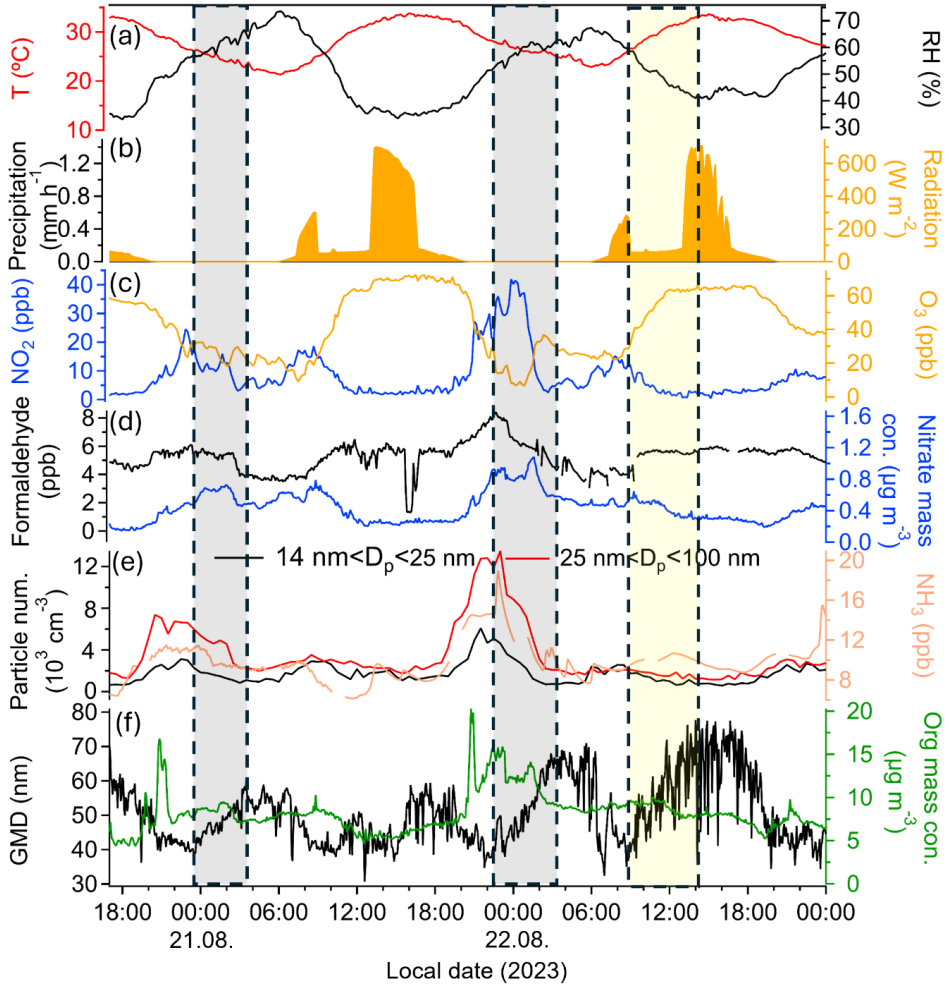

Figure 8. Meteorological parameters and gas-phase tracers during representative summer UFP growth events. Panels show (a) temperature (T) and relative humidity (RH), (b) precipitation and solar radiation*, (c) NO_2 and O_3, (d) formaldehyde and nitrate mass concentration, (e) number concentrations of 14-25 nm, 25-100 nm particles, and ammonia (f) geometric mean diameter (GMD) and total organic mass concentration. Grey shaded regions denote nighttime non-nucleation UFP growth events; the yellow shaded region indicates a daytime growth event. *Please note that the global radiation plotted here is affected by the shadow of the nearby buildings and is thus not representative for the whole street canyon of Theresienstrasse.

Winter UFP evolution is tightly controlled by meteorological conditions that favour the accumulation and condensation of primary combustion-related vapours. All UFP growth periods occur during nighttime and early morning, when solar radiation is absent, temperatures drop, and RH increases (Fig. 9a-b). These conditions coincide with a shallow boundary layer (Fig. 5f), which allows primary pollutants to build up rapidly near the surface. Correspondingly, NO_2 concentrations rise sharply while O_3 remains low (Fig. 9c), indicating intense traffic and residential combustion emissions coupled with minimal photochemical activity. This meteorological pattern aligns closely with the chemical composition shown in Figure 5, which reveals that winter UFP number

https://doi.org/10.5194/egusphere-2026-2195
Preprint. Discussion started: 19 May 2026

peaks correlate strongly with organic aerosol from traffic (R = 0.75), cooking (R = 0.69), and particularly nighttime-aged BBOA (R = 0.86). These correlations suggest that combustion-related emissions provide both the primary ultrafine particles and the semi-volatile organic vapours that contribute to subsequent particle growth. Multi-city analyses across urban Europe have shown that road traffic is the dominant source of urban UFP number concentrations, with additional contributions from residential combustion and, in some settings, cooking-related emissions, especially during stagnant conditions and reduced dilution (Ma et al., 2023; Garcia-Marles et al., 2024b; Rowell et al., 2024).

Figure 9 further clarifies the growth mechanism. Following the peaks in UFP number concentrations, the mean particle size increases while particle number concentrations decrease, indicating particle growth through condensation and coagulation processes. During these periods, neither formaldehyde nor total organic mass shows sharp increases (Fig. 9d, f), suggesting that growth is not driven by fresh photochemical SOA production but rather by the condensation of semi-volatile vapours already present in the air mass and accumulated within the shallow nocturnal boundary layer. Likewise, nitrate concentrations (Fig. 9d) show no coherent enhancement with mean particle size growth, indicating that inorganic pathways play a minor role. Similarly, NH_3 concentrations increase during the preceding emission accumulation periods but do not exhibit a clear relationship with the particle growth phase itself (Fig. 9e), suggesting that NH_3-driven ammonium nitrate formation is unlikely to be the dominant driver of the observed particle growth.

https://doi.org/10.5194/egusphere-2026-2195
Preprint. Discussion started: 19 May 2026

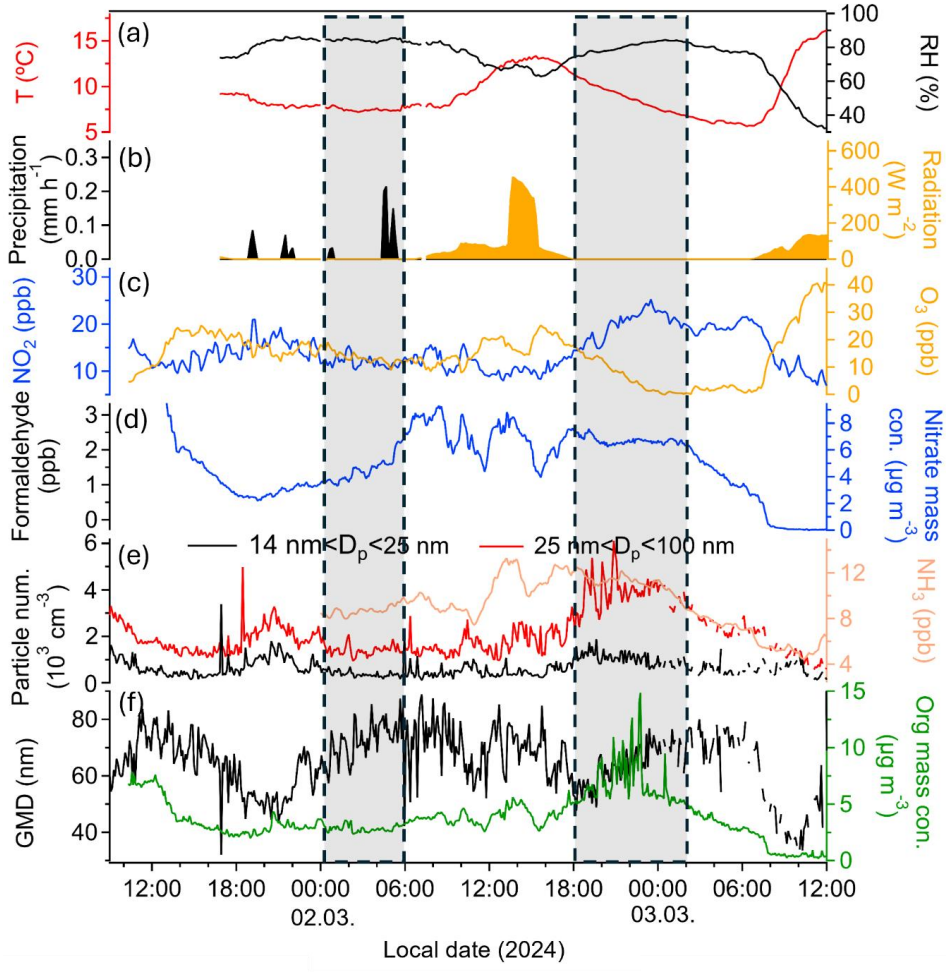

Figure 9. Meteorological parameters and gas-phase tracers during short-time winter UFP growth events. Panels show (a) temperature (T) and relative humidity (RH), (b) precipitation and solar radiation, (c) NO_2 and O_3, (d) formaldehyde and nitrate mass concentration, (e) number concentrations of 14-25 nm, 25-100 nm particles and ammonia (f) geometric mean diameter (GMD) and total organic mass concentration. Grey shaded regions denote nighttime non-nucleation UFP growth events.

Spring UFP evolution is shaped by a combination of nighttime boundary-layer stagnation and moderate daytime photochemical activity. As in other seasons, the largest UFP number peaks occur during nighttime and early morning (grey shading in Figure 10), when temperature decreases, RH increases, and solar radiation is zero (Fig. 10a-b). During these periods the boundary layer is shallow (Fig. 6f), allowing NO_2 to accumulate and O_3 to remain relatively low (Fig. 10c). Correspondingly, UFP numbers rise sharply (Fig. 10e), consistent with the primary-emission correlations in spring (traffic OA R = 0.74; cooking OA R = 0.70; Table S3) and the temporal patterns in Figure 6. Following these nighttime number peaks, the mean particle size increases while particle number concentration declines, indicating particle growth through condensation and coagulation processes, similar to the nocturnal growth pattern observed in summer and winter. Unlike winter, spring also exhibits distinct daytime

https://doi.org/10.5194/egusphere-2026-2195
Preprint. Discussion started: 19 May 2026

growth episodes (yellow shading in figure 10), marked by rising solar radiation and increasing O_3 accompanied by decreasing NO_2 (Fig. 10a-c). During these intervals the UFP number concentration does not show an increase, but the mean particle size rises sharply (Fig. 10e-f). This behaviour indicates efficient growth of pre-existing particles due to enhanced photochemical activity. The corresponding midday increase in aged BBOA in Figure 6 demonstrates that spring has a measurable contribution from photochemically oxidized organic vapours, although less intense than in summer. At the same time, nitrate concentrations remain relatively stable during both nighttime and daytime growth periods and do not show a clear concurrent increase with particle size growth, suggesting that inorganic nitrate condensation is unlikely to be the dominant driver. Similarly, NH_3 concentrations increase mainly during the preceding accumulation periods but show no clear relationship with the subsequent particle growth phase itself, indicating that NH_3-driven inorganic growth likely plays only a minor role. Overall, spring displays a mixed seasonal growth regime, combining summer and winter nighttime accumulation of primary emissions under a shallow boundary layer with summer-like daytime photochemical growth driven by oxidized organic vapours. This transitional behaviour suggests that spring UFP evolution reflects the coexistence of combustion-related nocturnal growth and photochemistry-enhanced daytime growth. Urban observations in Beijing show that spring UFP concentrations are influenced by both primary emissions and secondary formation, reflecting the transition from wintertime particle growth to the increasing occurrence of new particle formation events typical of summer (Li et al., 2023b). This parallel seasonal transition, observed despite the large differences in emission magnitude, suggests that the shift from combustion-dominated nocturnal growth in winter to photochemically enhanced daytime growth in spring may be a general feature of mid-latitude urban environments rather than a city-specific phenomenon.

https://doi.org/10.5194/egusphere-2026-2195
Preprint. Discussion started: 19 May 2026

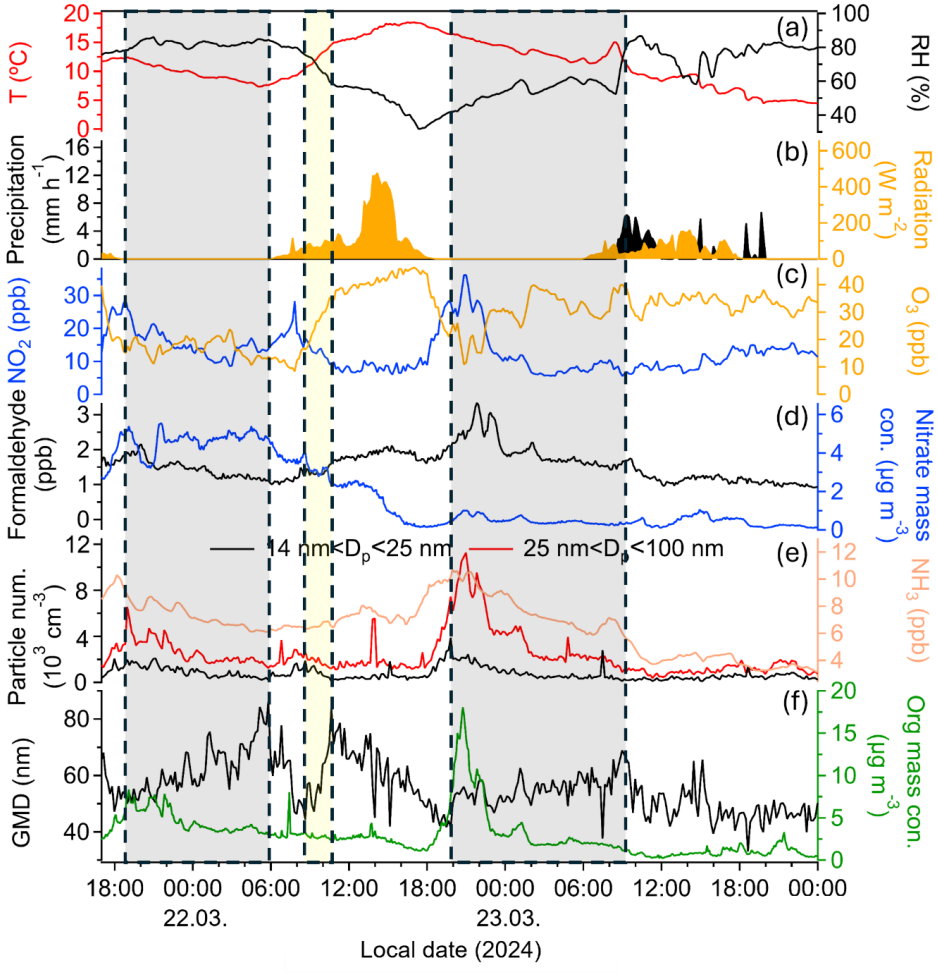

Figure 10. Meteorological parameters and gas-phase tracers during representative spring UFP growth events. Panels show (a) temperature (T) and relative humidity (RH), (b) precipitation and solar radiation, (c) NO_2 and O_3, (d) formaldehyde and nitrate mass concentration, (e) number concentrations of 14-25 nm, 25-100 nm particles and ammonia (f) geometric mean diameter (GMD) and total organic mass concentration. Grey shaded regions denote nighttime non-nucleation UFP growth events; the yellow shaded region indicates a daytime growth event.

Taking together the seasonal analyses above, a consistent mechanistic picture emerges. UFP number concentrations peak primarily under shallow boundary-layer conditions that trap traffic- and cooking-related emissions, with elevated NO_2 and reduced O_3. Such accumulation under stagnant nocturnal boundary layers has also been widely reported in urban environments, where suppressed mixing enhances the influence of primary emissions on ultrafine particle number concentrations (Mohan et al., 2024). These stagnant nighttime periods produce strong pre-growth number peaks in summer, winter, and spring. In contrast, mean particle size (GMD) growth is consistently decoupled from number concentration and is driven by the availability of condensable organic vapours, consistent with previous studies showing that particle growth is primarily controlled by condensable vapours rather than by primary particle emissions themselves (Mohr et al., 2019; Li et al., 2022). In

https://doi.org/10.5194/egusphere-2026-2195
Preprint. Discussion started: 19 May 2026

summer, growth arises from LV-OOA, BOA, and BBOA at night and from photochemically oxidized vapours during daytime, reflecting the strong role of photochemical oxidation and secondary organic aerosol formation under high radiation conditions reported for many urban atmospheres (Gu et al., 2023; Song et al., 2024). Winter growth relies almost entirely on condensation of semi-volatile biomass-burning and combustion organics accumulated in the very shallow nocturnal boundary layer, with negligible photochemical contribution, similar to observations in polluted wintertime urban environments were limited photochemistry shifts particle growth toward condensation of primary or semi-volatile combustion emissions (Sun et al., 2013; Li et al., 2023b). Spring exhibits a hybrid behaviour: nighttime growth resembles winter, while moderate daytime photochemistry enables additional oxidation-driven growth. Such transitional behaviour between winter accumulation regimes and summer photochemical regimes has also been observed in other mid-latitude urban environments (Li et al., 2023b). These results highlight that UFP numbers are controlled primarily by boundary-layer dynamics and primary emissions, whereas growth of mean particle size reflects seasonally varying sources of condensable organic vapours.

4 Conclusions

This study addressed key gaps regarding the sources, seasonal drivers, and atmospheric processes governing UFP in urban environments. Previous work has highlighted the diversity of UFP sources and the large spatial and temporal variability of particle number concentrations across cities (Kumar et al., 2014; Brines et al., 2015). However, limited chemical resolution and inconsistent measurement protocols have hindered a mechanistic understanding of how primary emissions, atmospheric oxidation, and meteorology jointly shape UFP number concentrations and size evolution. By combining particle number and size distribution measurements with aerosol particle and VOC composition, this work provides an integrated, high-resolution characterization of UFP dynamics across seasons in a street canyon of a typical European city, directly responding to the WHO/EU emphasis on improved UFP assessment.

Our results reveal a consistent two-step mechanism across all seasons: (1) reduce nighttime boundary-layer heights drive increasing UFP number concentrations through the accumulation of traffic, cooking and combustion related emissions (Ma et al., 2023; Garcia-Marles et al., 2024b; Rowell et al., 2024), and (2) subsequent particle growth from ~ 40 to 60 - 80 nm is governed by condensation of seasonally varying organic vapours, with new particle formation playing a negligible role across all seasons as evidenced by stable or declining particle number concentrations during growth periods. This finding extends previous observations of urban UFP variability by showing that particle number concentrations and particle growth processes are mechanistically decoupled, consistent with recent studies highlighting the dominant role of condensable organic vapours in particle growth (Man et al., 2015; Carnerero et al., 2018).

These results establish a unified mechanistic framework in which UFP dynamics in urban street canyons are governed by two independent controls: boundary layer modulated emission accumulation sets the number concentration, while the volatility and availability of organic vapours determines the extent and pathway of size growth. Seasonal differences in growth pathways further refine the conceptual understanding of UFP processes. In summer, growth is driven by both semi-volatile organics at night and photochemically oxidized vapours during daytime. In winter, growth is almost entirely controlled by biomass-burning and combustion-derived semi-volatile

https://doi.org/10.5194/egusphere-2026-2195
Preprint. Discussion started: 19 May 2026

organics accumulated in a very shallow nocturnal boundary layer, with negligible photochemical influence. Spring represents a transitional regime in which nighttime behaviour resembles winter while moderate daytime oxidation introduces an additional, weaker photochemical growth pathway. Such seasonal transitions between winter accumulation regimes and summer photochemical regimes have also been reported in other urban environments, including Beijing (Li et al., 2023b), and help explain the strong seasonal heterogeneity in urban UFP characteristics reported across Europe (Giemsa et al., 2021; Garcia-Marles et al., 2024b).

By directly linking UFP size evolution with chemically resolved OA/SVOA/VOC factors and meteorological drivers, this study demonstrates that UFP number concentrations are primarily determined by emission strength and boundary-layer dynamics, whereas UFP growth is dominated by the availability and volatility of organic vapours rather than by nucleation events. This mechanistic decoupling between number concentration and size growth has not been explicitly demonstrated across three seasons in a European street canyon before. While Garcia-Marles et al. (2024b) identified traffic and photonucleation as dominant UFP sources across European cities, our results show that condensation of semi-volatile organics rather than nucleation governs size growth in Munich across all seasons, extending the current understanding of UFP processes in urban street canyons. Furthermore, the absence of classical new particle formation in all observed growth events contrasts with studies in more polluted Asian megacities such as Beijing, where NPF contributed substantially to UFP number concentrations across seasons (Tao et al., 2023; Li et al., 2023b), highlighting the importance of city-specific emission profiles and condensation sink conditions in shaping UFP dynamics.

Several caveats should be considered when interpreting these results. The aerosol composition measurements primarily reflect the accumulation mode, and future work combining single-particle mass spectrometry with high-time-resolution volatility measurements would further constrain the role of individual organic compounds in UFP growth. From a modelling perspective, the mechanistic decoupling demonstrated here suggests that separate treatment of boundary-layer-driven accumulation and organics-driven condensational growth is necessary for accurate representation of UFP in urban street canyons, rather than treating number concentration and size as co-varying quantities. The dominance of condensational growth over new particle formation across all seasons also implies that the condensation sink is a key variable for UFP modelling in European cities, in contrast to the NPF-dominated regimes reported in Asian megacities.

These findings have direct implications for mitigation strategies targeting urban UFP exposure. First, since UFP number concentrations are primarily driven by traffic and cooking emissions accumulating under shallow boundary layers, measures targeting these primary emission sources are most effective for reducing peak UFP exposure. Stricter vehicle emission standards targeting sub-23 nm non-volatile particles, which dominate traffic emissions as shown by Lintusaari et al. (2023), and the adoption of advanced diesel particle filters represent critical near-term interventions, though their effectiveness in reducing nucleation-mode UFPs remains limited (Damayanti et al., 2023). Emission controls on commercial cooking, such as improved ventilation and filtration systems in restaurant-dense urban areas, should also be considered given the consistently strong correlation between cooking OA and UFP number concentrations observed across all seasons. Second, since UFP growth in summer is strongly driven by condensable organic vapours from biomass burning and photochemical oxidation, reducing open biomass burning and controlling VOC emissions from both traffic and biomass burning sources would limit the availability of condensable material for particle growth. In winter, when biomass-burning SVOA

https://doi.org/10.5194/egusphere-2026-2195
Preprint. Discussion started: 19 May 2026

dominates UFP growth, targeted restrictions on residential wood burning, as already implemented in several European cities, would be particularly effective (Roig Rodelas et al., 2019). Third, the strong seasonal dependence of UFP drivers identified here underscores that a one-size-fits-all approach to UFP mitigation is insufficient. Season-specific strategies are needed: summer interventions should prioritize VOC emission controls and photochemical oxidant reduction, while winter measures should focus on combustion emission restrictions and boundary-layer ventilation through urban planning. These results directly support the WHO and EU policy framework calling for improved UFP monitoring and source-specific exposure reduction, and provide a seasonally resolved mechanistic basis for designing targeted urban air quality interventions.

Data availability

Data corresponding to this manuscript will be available at the data repository KITopen (DOI:10.35097/bs139dd72d5s0r6a). The authors are willing to provide additional information for data that may be of interest to readers upon request.

Supplement

The supplement related to this article is available online at Atmospheric Chemistry and Physics (ACP).

Author contributions

FK, JC, and HS conceived the concept, planned, and organized the campaign. YXL did the AMS and PTR-MS measurements, analyzed most of the data and wrote the manuscript with contributions from all co-authors. HS planned and organized the measurements, took care of the particle number, size and additional trace gas measurements. HZ, SA, AW, JC and FK supported instrument set up and conducted lidar measurements. XS, YWL and FK checked and calibrated the instruments during the measurements. JBS, ZA, and JS contributed to data analysis. TL contributed to planning of the measurement campaign and reviewed the manuscript.

Competing interests

Two co-authors are co-editors of ACP but the authors declare that there is no conflict of interests.

Acknowledgements

We gratefully acknowledge the support by the meteorological department of the Ludwig-Maximilians-University of Munich (Group of Prof. Bernhard Mayer) and especially Markus Garhammer. The support by the technical team (Group of Steffen Vogt) of the Institute of Meteorology and Climate Research Atmospheric Aerosol Research of the Karlsruhe Institute of Technology was extremely helpful.

https://doi.org/10.5194/egusphere-2026-2195
Preprint. Discussion started: 19 May 2026

Financial support

The China Scholarship Council (CSC) provided PhD scholarships for Yanxia Li and Xuefeng Shi. The KIT Graduate School for Climate and Environment (GRACE) supported Yanxia Li. The KIT funded the campaign in the program "Changing Earth – Sustaining our Future" of the Helmholtz Association. The campaign was partly funded by the Institute for Advanced Study, Technical University of Munich (Grant no. 291763). The TUM authors are partly supported by ERC Consolidator Grant CoSense4Climate (Grant 101089203) and Bavarian State Ministry of the Environment (Grant TLK 01U-75487). Yaowei Li acknowledges partial support from the NOAA Climate and Global Change Postdoctoral Fellowship Program, administered by UCAR's Cooperative Programs for the Advancement of Earth System Science (CPAESS) under award #NA23OAR4310383B

5 References

Abbou, G., Ghersi, V., Gaie-Levrel, F., Kauffmann, A., Reynaud, M., Debert, C., Quénel, P., and Baudic, A.: Ultrafine Particles Monitoring in Paris: From Total Number Concentrations to Size Distributions Measurements, Aerosol and Air Quality Research, 24, 10.4209/aaqr.240093, 2024.

Abdillah, S. F. I., You, S.-J., and Wang, Y.-F.: Characterizing Traffic-Related Ultrafine Particles in Roadside Microenvironments: Spatiotemporal Insights from Industrial Parks, Aerosol and Air Quality Research, 24, 10.4209/aaqr.230295, 2024.

Ahn, H., Lee, J., and Hong, A.: Does urban greenway design affect air pollution exposure? A case study of Seoul, South Korea, Sustainable Cities and Society, 72, 10.1016/j.scs.2021.103038, 2021.

Ajith, T. C., Windwer, E., Li, C., Fang, Z., Kompalli, S. K., Nursanto, F. R., Olayemi, T. E., Ese, J. I., Sharpe, S. A. L., Fraund, M., Moffet, R. C., Laskin, A., Fry, J. L., and Rudich, Y.: Investigating New Particle Formation and Growth Over an Urban Location in the Eastern Mediterranean, J Geophys Res Atmos, 129, e2024JD041802, 10.1029/2024JD041802, 2024.

Aktypis, A., Sippial, D. J., Vasilakopoulou, C. N., Matrali, A., Kaltsonoudis, C., Simonati, A., Paglione, M., Rinaldi, M., Decesari, S., and Pandis, S. N.: Formation and chemical evolution of secondary organic aerosol in two different environments: a dual-chamber study, Atmospheric Chemistry and Physics, 24, 13769-13791, 10.5194/acp-24-13769-2024, 2024.

Andreae, M. O., Andreae, T. W., Ditas, F., and Pöhlker, C.: Frequent new particle formation at remote sites in the subboreal forest of North America, Atmospheric Chemistry and Physics, 22, 2487-2505, 10.5194/acp-22-2487-2022, 2022.

The Legislative Framework for Ultrafine Particles in Europe: https://www.avl.com/en-de/expert-article/legislative-framework-ultrafine-particles-europe, last access: 13 October 2025.

Birmili, W., Heinke, K., Pitz, M., Matschullat, J., Wiedensohler, A., Cyrys, J., Wichmann, H. E., and Peters, A.: Particle number size distributions in urban air before and after volatilisation, Atmospheric Chemistry and Physics, 10, 4643-4660, 10.5194/acp-10-4643-2010, 2010.

Bousiotis, D., Singh, A., Haugen, M., Beddows, D. C. S., Diez, S., Murphy, K. L., Edwards, P. M., Boies, A., Harrison, R. M., and Pope, F. D.: Assessing the sources of particles at an urban background site using both regulatory instruments and low-cost sensors – a comparative study, Atmospheric Measurement Techniques, 14, 4139-4155, 10.5194/amt-14-4139-2021, 2021a.

https://doi.org/10.5194/egusphere-2026-2195
Preprint. Discussion started: 19 May 2026

Bousiotis, D., Pope, F. D., Beddows, D. C. S., Dall'Osto, M., Massling, A., Nøjgaard, J. K., Nordstrøm, C., Niemi, J. V., Portin, H., Petäjä, T., Perez, N., Alastuey, A., Querol, X., Kouvarakis, G., Mihalopoulos, N., Vratolis, S., Eleftheriadis, K., Wiedensohler, A., Weinhold, K., Merkel, M., Tuch, T., and Harrison, R. M.: A phenomenology of new particle formation (NPF) at 13 European sites, Atmospheric Chemistry and Physics, 21, 11905-11925, 10.5194/acp-21-11905-2021, 2021b.

Brean, J., Rowell, A., Beddows, D. C. S., Weinhold, K., Mettke, P., Merkel, M., Tuch, T., Rissanen, M., Maso, M. D., Kumar, A., Barua, S., Iyer, S., Karppinen, A., Wiedensohler, A., Shi, Z., and Harrison, R. M.: Road Traffic Emissions Lead to Much Enhanced New Particle Formation through Increased Growth Rates, Environ Sci Technol, 58, 10664-10674, 10.1021/acs.est.3c10526, 2024.

Brean, J., Bortolussi, F., Rowell, A., Beddows, D. C. S., Weinhold, K., Mettke, P., Merkel, M., Kumar, A., Barua, S., Iyer, S., Karppinen, A., Sandstrom, H., Rinke, P., Wiedensohler, A., Pohlker, M., Dal Maso, M., Rissanen, M., Shi, Z., and Harrison, R. M.: Traffic-Emitted Amines Promote New Particle Formation at Roadsides, ACS EST Air, 2, 1704-1713, 10.1021/acsestair.5c00119, 2025.

Brines, M., Dall'Osto, M., Beddows, D. C. S., Harrison, R. M., Gómez-Moreno, F., Núñez, L., Artíñano, B., Costabile, F., Gobbi, G. P., Salimi, F., Morawska, L., Sioutas, C., and Querol, X.: Traffic and nucleation events as main sources of ultrafine particles in high-insolation developed world cities, Atmospheric Chemistry and Physics, 15, 5929-5945, 10.5194/acp-15-5929-2015, 2015.

Carnerero, C., Pérez, N., Reche, C., Ealo, M., Titos, G., Lee, H.-K., Eun, H.-R., Park, Y.-H., Dada, L., Paasonen, P., Kerminen, V.-M., Mantilla, E., Escudero, M., Gómez-Moreno, F. J., Alonso-Blanco, E., Coz, E., Saiz-Lopez, A., Temime-Roussel, B., Marchand, N., Beddows, D. C. S., Harrison, R. M., Petäjä, T., Kulmala, M., Ahn, K.-H., Alastuey, A., and Querol, X.: Vertical and horizontal distribution of regional new particle formation events in Madrid, Atmospheric Chemistry and Physics, 18, 16601-16618, 10.5194/acp-18-16601-2018, 2018.

Carrillo-Cardenas, G., Hoch, S. W., Pardyjak, E., Garcia, M., Brown, W., Pu, Z., and Hallar, A. G.: Elucidating New Particle Formation in Complex Terrain During the Winter 2022 Cold Fog Amongst Complex Terrain (CFACT) Campaign, Journal of Geophysical Research: Atmospheres, 130, 10.1029/2024jd042307, 2025.

Chen, T. L., Hsiao, T. C., Chuang, H. C., Ting, Y. C., and Wang, C. H.: A mobile platform for characterizing on-road tailpipe emissions and toxicity of ultrafine particles under real driving Conditions, Environ Res, 216, 114523, 10.1016/j.envres.2022.114523, 2023.

Cohen, M. D., Stunder, B. J. B., Rolph, G. D., Draxler, R. R., Stein, A. F., and Ngan, F.: NOAA's HYSPLIT Atmospheric Transport and Dispersion Modeling System, Bulletin of the American Meteorological Society, 96, 2059-2077, 10.1175/bams-d-14-00110.1, 2015.

Dall'Osto, M., Querol, X., Alastuey, A., O'Dowd, C., Harrison, R. M., Wenger, J., and Gómez-Moreno, F. J.: On the spatial distribution and evolution of ultrafine particles in Barcelona, Atmospheric Chemistry and Physics, 13, 741-759, 10.5194/acp-13-741-2013, 2013.

Damayanti, S., Harrison, R. M., Pope, F., and Beddows, D. C. S.: Limited impact of diesel particle filters on road traffic emissions of ultrafine particles, Environ Int, 174, 107888, 10.1016/j.envint.2023.107888, 2023.

de Jesus, A. L., Rahman, M. M., Mazaheri, M., Thompson, H., Knibbs, L. D., Jeong, C., Evans, G., Nei, W., Ding, A., Qiao, L., Li, L., Portin, H., Niemi, J. V., Timonen, H., Luoma, K., Petaja, T., Kulmala, M., Kowalski, M., Peters, A., Cyrys, J., Ferrero, L., Manigrasso, M., Avino, P., Buonano, G., Reche, C., Querol, X., Beddows, D., Harrison, R. M., Sowlat, M. H., Sioutas, C., and Morawska, L.: Ultrafine particles and PM(2.5) in the air of

https://doi.org/10.5194/egusphere-2026-2195
Preprint. Discussion started: 19 May 2026

cities around the world: Are they representative of each other?, Environ Int, 129, 118-135, 10.1016/j.envint.2019.05.021, 2019.

Flood-Garibay, J. A., Angulo-Molina, A., and Mendez-Rojas, M. A.: Particulate matter and ultrafine particles in urban air pollution and their effect on the nervous system, Environ Sci Process Impacts, 25, 704-726, 10.1039/d2em00276k, 2023.

Folwarczny, E., Forster, F., Jörres, R. A., Rakete, S., Ye, S., Wenig, M., Gawlitta, N., Schnelle-Kreis, J., Winterhalter, R., Müller, A., Nowak, D., and Karrasch, S.: Acute health effects of ambient air pollution including ultrafine particles in a semi-experimental setting in young, healthy individuals, Particle and Fibre Toxicology, 22, 14, 10.1186/s12989-025-00628-7, 2025.

Garcia-Marles, M., Lara, R., Reche, C., Perez, N., Tobias, A., Savadkoohi, M., Beddows, D., Salma, I., Vorosmarty, M., Weidinger, T., Hueglin, C., Mihalopoulos, N., Grivas, G., Kalkavouras, P., Ondracek, J., Zikova, N., Niemi, J. V., Manninen, H. E., Green, D. C., Tremper, A. H., Norman, M., Vratolis, S., Eleftheriadis, K., Gomez-Moreno, F. J., Alonso-Blanco, E., Wiedensohler, A., Weinhold, K., Merkel, M., Bastian, S., Hoffmann, B., Altug, H., Petit, J. E., Favez, O., Dos Santos, S. M., Putaud, J. P., Dinoi, A., Contini, D., Timonen, H., Lampilahti, J., Petaja, T., Pandolfi, M., Hopke, P. K., Harrison, R. M., Alastuey, A., and Querol, X.: Inter-annual trends of ultrafine particles in urban Europe, Environ Int, 185, 108510, 10.1016/j.envint.2024.108510, 2024a.

Garcia-Marles, M., Lara, R., Reche, C., Perez, N., Tobias, A., Savadkoohi, M., Beddows, D., Salma, I., Vorosmarty, M., Weidinger, T., Hueglin, C., Mihalopoulos, N., Grivas, G., Kalkavouras, P., Ondracek, J., Zikova, N., Niemi, J. V., Manninen, H. E., Green, D. C., Tremper, A. H., Norman, M., Vratolis, S., Diapouli, E., Eleftheriadis, K., Gomez-Moreno, F. J., Alonso-Blanco, E., Wiedensohler, A., Weinhold, K., Merkel, M., Bastian, S., Hoffmann, B., Altug, H., Petit, J. E., Acharja, P., Favez, O., Santos, S. M. D., Putaud, J. P., Dinoi, A., Contini, D., Casans, A., Casquero-Vera, J. A., Crumeyrolle, S., Bourrianne, E., Poppel, M. V., Dreesen, F. E., Harni, S., Timonen, H., Lampilahti, J., Petaja, T., Pandolfi, M., Hopke, P. K., Harrison, R. M., Alastuey, A., and Querol, X.: Source apportionment of ultrafine particles in urban Europe, Environ Int, 194, 109149, 10.1016/j.envint.2024.109149, 2024b.

Giemsa, E., Soentgen, J., Kusch, T., Beck, C., Münkel, C., Cyrys, J., and Pitz, M.: Influence of Local Sources and Meteorological Parameters on the Spatial and Temporal Distribution of Ultrafine Particles in Augsburg, Germany, Frontiers in Environmental Science, 8, 10.3389/fenvs.2020.609846, 2021.

Gu, Y., Huang, R.-J., Duan, J., Xu, W., Lin, C., Zhong, H., Wang, Y., Ni, H., Liu, Q., Xu, R., Wang, L., and Li, Y. J.: Multiple pathways for the formation of secondary organic aerosol in the North China Plain in summer, Atmospheric Chemistry and Physics, 23, 5419-5433, 10.5194/acp-23-5419-2023, 2023.

Guo, S., Hu, M., Peng, J., Wu, Z., Zamora, M. L., Shang, D., Du, Z., Zheng, J., Fang, X., Tang, R., Wu, Y., Zeng, L., Shuai, S., Zhang, W., Wang, Y., Ji, Y., Li, Y., Zhang, A. L., Wang, W., Zhang, F., Zhao, J., Gong, X., Wang, C., Molina, M. J., and Zhang, R.: Remarkable nucleation and growth of ultrafine particles from vehicular exhaust, Proc Natl Acad Sci U S A, 117, 3427-3432, 10.1073/pnas.1916366117, 2020.

Haeffelin, M., Ribaud, J.-F., Céspedes, J., Dupont, J.-C., Lemonsu, A., Masson, V., Nagel, T., and Kotthaus, S.: Impact of boundary layer stability on urban park cooling effect intensity, Atmospheric Chemistry and Physics, 24, 14101-14122, 10.5194/acp-24-14101-2024, 2024.

https://doi.org/10.5194/egusphere-2026-2195
Preprint. Discussion started: 19 May 2026

Hama, S. M. L., Cordell, R. L., and Monks, P. S.: Quantifying primary and secondary source contributions to ultrafine particles in the UK urban background, Atmospheric Environment, 166, 62-78, 10.1016/j.atmosenv.2017.07.013, 2017.

Hao, L., Garmash, O., Ehn, M., Miettinen, P., Massoli, P., Mikkonen, S., Jokinen, T., Roldin, P., Aalto, P., Yli-Juuti, T., Joutsensaari, J., Petäjä, T., Kulmala, M., Lehtinen, K. E. J., Worsnop, D. R., and Virtanen, A.: Combined effects of boundary layer dynamics and atmospheric chemistry on aerosol composition during new particle formation periods, Atmospheric Chemistry and Physics, 18, 17705-17716, 10.5194/acp-18-17705-2018, 2018.

Hirshorn, N. S., Zuromski, L. M., Rapp, C., McCubbin, I., Carrillo-Cardenas, G., Yu, F., and Hallar, A. G.: Seasonal significance of new particle formation impacts on cloud condensation nuclei at a mountaintop location, Atmospheric Chemistry and Physics, 22, 15909-15924, 10.5194/acp-22-15909-2022, 2022.

Kecorius, S., Madueño, L., Plauškaitė, K., Byčenkienė, S., Lovrić, M., Petrić, V., Carranza-García, M., Jiménez-Navarro, M. J., Martínez-Ballesteros, M. d. M., and Kecorius, G.: Road-traffic emissions of ultrafine particles and elemental black carbon in six Northern European cities, Environmental Advances, 21, 10.1016/j.envadv.2025.100661, 2025.

Kim, S., Machesky, J., Gentner, D. R., and Presto, A. A.: Real-world observations of reduced nitrogen and ultrafine particles in commercial cooking organic aerosol emissions, Atmospheric Chemistry and Physics, 24, 1281-1298, 10.5194/acp-24-1281-2024, 2024.

Kumar, P., Morawska, L., Birmili, W., Paasonen, P., Hu, M., Kulmala, M., Harrison, R. M., Norford, L., and Britter, R.: Ultrafine particles in cities, Environ Int, 66, 1-10, 10.1016/j.envint.2014.01.013, 2014.

Lepisto, T., Barreira, L. M. F., Helin, A., Niemi, J. V., Kuittinen, N., Lintusaari, H., Silvonen, V., Markkula, L., Manninen, H. E., Timonen, H., Jalava, P., Saarikoski, S., and Ronkko, T.: Snapshots of wintertime urban aerosol characteristics: Local sources emphasized in ultrafine particle number and lung deposited surface area, Environ Res, 231, 116068, 10.1016/j.envres.2023.116068, 2023.

Li, Q.-Q., Guo, Y.-T., Yang, J.-Y., and Liang, C.-S.: Review on main sources and impacts of urban ultrafine particles: Traffic emissions, nucleation, and climate modulation, Atmospheric Environment: X, 19, 10.1016/j.aeaoa.2023.100221, 2023a.

Li, X., Chen, Y., Li, Y., Cai, R., Li, Y., Deng, C., Wu, J., Yan, C., Cheng, H., Liu, Y., Kulmala, M., Hao, J., Smith, J. N., and Jiang, J.: Seasonal variations in composition and sources of atmospheric ultrafine particles in urban Beijing based on near-continuous measurements, Atmospheric Chemistry and Physics, 23, 14801-14812, 10.5194/acp-23-14801-2023, 2023b.

Li, X., Li, Y., Cai, R., Yan, C., Qiao, X., Guo, Y., Deng, C., Yin, R., Chen, Y., Li, Y., Yao, L., Sarnela, N., Zhang, Y., Petaja, T., Bianchi, F., Liu, Y., Kulmala, M., Hao, J., Smith, J. N., and Jiang, J.: Insufficient Condensable Organic Vapors Lead to Slow Growth of New Particles in an Urban Environment, Environ Sci Technol, 56, 9936-9946, 10.1021/acs.est.2c01566, 2022.

Li, Y., Zhang, H., Shi, X., Li, Y., Abou-Rizk, S., Smith, J., An, Z., Wenzel, A., Song, J., Leisner, T., Keutsch, F., Chen, J., and Saathoff, H.: Sources, concentrations, and seasonal variations of VOC and aerosol particles in downtown Munich in 2023/24, EGUsphere [preprint], https://doi.org/10.5194/egusphere-2025-5191, 2026.

https://doi.org/10.5194/egusphere-2026-2195
Preprint. Discussion started: 19 May 2026

Li, Z., Guo, J., Ding, A., Liao, H., Liu, J., Sun, Y., Wang, T., Xue, H., Zhang, H., and Zhu, B.: Aerosol and boundary-layer interactions and impact on air quality, National Science Review, 4, 810-833, 10.1093/nsr/nwx117, 2017.

Liaskoni, M., Huszár, P., Bartík, L., Prieto Perez, A. P., Karlický, J., and Šindelářová, K.: The long-term impact of biogenic volatile organic compound emissions on urban ozone patterns over central Europe: contributions from urban and rural vegetation, Atmospheric Chemistry and Physics, 24, 13541-13569, 10.5194/acp-24-13541-2024, 2024.

Lintusaari, H., Kuuluvainen, H., Vanhanen, J., Salo, L., Portin, H., Jarvinen, A., Juuti, P., Hietikko, R., Teinila, K., Timonen, H., Niemi, J. V., and Ronkko, T.: Sub-23 nm Particles Dominate Non-Volatile Particle Number Emissions of Road Traffic, Environ Sci Technol, 57, 10763-10772, 10.1021/acs.est.3c03221, 2023.

Ma, N. and Birmili, W.: Estimating the contribution of photochemical particle formation to ultrafine particle number averages in an urban atmosphere, Sci Total Environ, 512-513, 154-166, 10.1016/j.scitotenv.2015.01.009, 2015.

Ma, T., Furutani, H., Duan, F., Ma, Y., Toyoda, M., Kimoto, T., Huang, T., and He, K.: Real-Time Single-Particle Characteristics and Aging of Cooking Aerosols in Urban Beijing, Environmental Science & Technology Letters, 10, 404-409, 10.1021/acs.estlett.3c00053, 2023.

Man, H., Zhu, Y., Ji, F., Yao, X., Lau, N. T., Li, Y., Lee, B. P., and Chan, C. K.: Comparison of daytime and nighttime new particle growth at the HKUST supersite in Hong Kong, Environ Sci Technol, 49, 7170-7178, 10.1021/acs.est.5b02143, 2015.

Meier, R., Eeftens, M., Aguilera, I., Phuleria, H. C., Ineichen, A., Davey, M., Ragettli, M. S., Fierz, M., Schindler, C., Probst-Hensch, N., Tsai, M. Y., and Kunzli, N.: Ambient ultrafine particle levels at residential and reference sites in urban and rural Switzerland, Environ Sci Technol, 49, 2709-2715, 10.1021/es505246m, 2015.

Mohan, V., Kumar Soni, V., and Kumar Mishra, R.: Analysing the impact of day-night road traffic variation on ultrafine particle number size distribution and concentration at an urban site in the megacity Delhi, Atmospheric Pollution Research, 15, 10.1016/j.apr.2024.102065, 2024.

Mohr, C., Thornton, J. A., Heitto, A., Lopez-Hilfiker, F. D., Lutz, A., Riipinen, I., Hong, J., Donahue, N. M., Hallquist, M., Petaja, T., Kulmala, M., and Yli-Juuti, T.: Molecular identification of organic vapors driving atmospheric nanoparticle growth, Nat Commun, 10, 4442, 10.1038/s41467-019-12473-2, 2019.

Ambient Ultrafine Particle Evidence for Policy Makers: https://efca.net/files/UFPs%20White%20Paper%20-%20FINAL.pdf, last access: 2025 October 15.

Muller, M., Eichler, P., D'Anna, B., Tan, W., and Wisthaler, A.: Direct Sampling and Analysis of Atmospheric Particulate Organic Matter by Proton-Transfer-Reaction Mass Spectrometry, Anal Chem, 89, 10889-10897, 10.1021/acs.analchem.7b02582, 2017.

Okuljar, M., Kuuluvainen, H., Kontkanen, J., Garmash, O., Olin, M., Niemi, J. V., Timonen, H., Kangasluoma, J., Tham, Y. J., Baalbaki, R., Sipilä, M., Salo, L., Lintusaari, H., Portin, H., Teinilä, K., Aurela, M., Dal Maso, M., Rönkkö, T., Petäjä, T., and Paasonen, P.: Measurement report: The influence of traffic and new particle formation on the size distribution of 1–800 nm particles in Helsinki – a street canyon and an urban background station comparison, Atmospheric Chemistry and Physics, 21, 9931-9953, 10.5194/acp-21-9931-2021, 2021.

https://doi.org/10.5194/egusphere-2026-2195
Preprint. Discussion started: 19 May 2026

Rattigan, O. V., Hassanzadeh, Y. T., Teora, A. C., Felton, H. D., Civerolo, K. L., Lance, S., Schwab, J. J., and Hopke, P. K.: Ultrafine particle measurements in New York State, Atmospheric Pollution Research, 15, 10.1016/j.apr.2024.102164, 2024.

Roig Rodelas, R., Chakraborty, A., Perdrix, E., Tison, E., and Riffault, V.: Real-time assessment of wintertime organic aerosol characteristics and sources at a suburban site in northern France, Atmospheric Environment, 203, 48-61, 10.1016/j.atmosenv.2019.01.035, 2019.

Rose, C., Collaud Coen, M., Andrews, E., Lin, Y., Bossert, I., Lund Myhre, C., Tuch, T., Wiedensohler, A., Fiebig, M., Aalto, P., Alastuey, A., Alonso-Blanco, E., Andrade, M., Artíñano, B., Arsov, T., Baltensperger, U., Bastian, S., Bath, O., Beukes, J. P., Brem, B. T., Bukowiecki, N., Casquero-Vera, J. A., Conil, S., Eleftheriadis, K., Favez, O., Flentje, H., Gini, M. I., Gómez-Moreno, F. J., Gysel-Beer, M., Hallar, A. G., Kalapov, I., Kalivitis, N., Kasper-Giebl, A., Keywood, M., Kim, J. E., Kim, S.-W., Kristensson, A., Kulmala, M., Lihavainen, H., Lin, N.-H., Lyamani, H., Marinoni, A., Martins Dos Santos, S., Mayol-Bracero, O. L., Meinhardt, F., Merkel, M., Metzger, J.-M., Mihalopoulos, N., Ondracek, J., Pandolfi, M., Pérez, N., Petäjä, T., Petit, J.-E., Picard, D., Pichon, J.-M., Pont, V., Putaud, J.-P., Reisen, F., Sellegri, K., Sharma, S., Schauer, G., Sheridan, P., Sherman, J. P., Schwerin, A., Sohmer, R., Sorribas, M., Sun, J., Tulet, P., Vakkari, V., van Zyl, P. G., Velarde, F., Villani, P., Vratolis, S., Wagner, Z., Wang, S.-H., Weinhold, K., Weller, R., Yela, M., Zdimal, V., and Laj, P.: Seasonality of the particle number concentration and size distribution: a global analysis retrieved from the network of Global Atmosphere Watch (GAW) near-surface observatories, Atmospheric Chemistry and Physics, 21, 17185-17223, 10.5194/acp-21-17185-2021, 2021.

Rowell, A., Brean, J., Beddows, D. C. S., Petäjä, T., Vörösmarty, M., Salma, I., Niemi, J. V., Manninen, H. E., van Pinxteren, D., Tuch, T., Weinhold, K., Shi, Z., and Harrison, R. M.: Insights into the sources of ultrafine particle numbers at six European urban sites obtained by investigating COVID-19 lockdowns, Atmospheric Chemistry and Physics, 24, 9515-9531, 10.5194/acp-24-9515-2024, 2024.

Saarikoski, S., Hellén, H., Praplan, A. P., Schallhart, S., Clusius, P., Niemi, J. V., Kousa, A., Tykkä, T., Kouznetsov, R., Aurela, M., Salo, L., Rönkkö, T., Barreira, L. M. F., Pirjola, L., and Timonen, H.: Characterization of volatile organic compounds and submicron organic aerosol in a traffic environment, Atmospheric Chemistry and Physics, 23, 2963-2982, 10.5194/acp-23-2963-2023, 2023.

Salimi, F., Rahman, M. M., Clifford, S., Ristovski, Z., and Morawska, L.: Nocturnal new particle formation events in urban environments, Atmospheric Chemistry and Physics, 17, 521-530, 10.5194/acp-17-521-2017, 2017.

Schraufnagel, D. E.: The health effects of ultrafine particles, Exp Mol Med, 52, 311-317, 10.1038/s12276-020-0403-3, 2020.

Simon, M. C., Hudda, N., Naumova, E. N., Levy, J. I., Brugge, D., and Durant, J. L.: Comparisons of Traffic-Related Ultrafine Particle Number Concentrations Measured in Two Urban Areas by Central, Residential, and Mobile Monitoring, Atmos Environ (1994), 169, 113-127, 10.1016/j.atmosenv.2017.09.003, 2017.

Song, J., Saathoff, H., Jiang, F., Gao, L., Zhang, H., and Leisner, T.: Sources of organic gases and aerosol particles and their roles in nighttime particle growth at a rural forested site in southwest Germany, Atmospheric Chemistry and Physics, 24, 6699-6717, 10.5194/acp-24-6699-2024, 2024.

Straaten, A., Meier, F., Scherer, D., and Weber, S.: Significant reduction of ultrafine particle emission fluxes to the urban atmosphere during the COVID-19 lockdown, Sci Total Environ, 838, 156516, 10.1016/j.scitotenv.2022.156516, 2022.

https://doi.org/10.5194/egusphere-2026-2195
Preprint. Discussion started: 19 May 2026

Sun, J., Hermann, M., Weinhold, K., Merkel, M., Birmili, W., Yang, Y., Tuch, T., Flentje, H., Briel, B., Ries, L., Couret, C., Elsasser, M., Sohmer, R., Wirtz, K., Meinhardt, F., Schütze, M., Bath, O., Hellack, B., Kerminen, V.-M., Kulmala, M., Ma, N., and Wiedensohler, A.: Measurement report: Contribution of atmospheric new particle formation to ultrafine particle concentration, cloud condensation nuclei, and radiative forcing – results from 5-year observations in central Europe, Atmospheric Chemistry and Physics, 24, 10667-10687, 10.5194/acp-24-10667-2024, 2024.

Sun, Y. L., Wang, Z. F., Fu, P. Q., Yang, T., Jiang, Q., Dong, H. B., Li, J., and Jia, J. J.: Aerosol composition, sources and processes during wintertime in Beijing, China, Atmospheric Chemistry and Physics, 13, 4577-4592, 10.5194/acp-13-4577-2013, 2013.

Tao, L., Zhou, Z., Tao, J., Zhang, L., Wu, C., Li, J., Yue, D., Wu, Z., Zhang, Z., Yuan, Z., Huang, J., and Wang, B.: High contribution of new particle formation to ultrafine particles in four seasons in an urban atmosphere in south China, Sci Total Environ, 889, 164202, 10.1016/j.scitotenv.2023.164202, 2023.

Teinilä, K., Saarikoski, S., Lintusaari, H., Lepistö, T., Marjanen, P., Aurela, M., Hellén, H., Tykkä, T., Lampimäki, M., Lampilahti, J., Barreira, L., Mäkelä, T., Kangas, L., Hatakka, J., Harni, S., Kuula, J., V. Niemi, J., Portin, H., Yli-Ojanperä, J., Niemelä, V., Jäppi, M., Lehtipalo, K., Vanhanen, J., Pirjola, L., Manninen, H. E., Petäjä, T., Rönkkö, T., and Timonen, H.: Measurement report: Wintertime aerosol characterization at an urban traffic site in Helsinki, Finland, Atmospheric Chemistry and Physics, 25, 4907-4928, 10.5194/acp-25-4907-2025, 2025.

Trechera, P., Garcia-Marles, M., Liu, X., Reche, C., Perez, N., Savadkoohi, M., Beddows, D., Salma, I., Vorosmarty, M., Casans, A., Casquero-Vera, J. A., Hueglin, C., Marchand, N., Chazeau, B., Gille, G., Kalkavouras, P., Mihalopoulos, N., Ondracek, J., Zikova, N., Niemi, J. V., Manninen, H. E., Green, D. C., Tremper, A. H., Norman, M., Vratolis, S., Eleftheriadis, K., Gomez-Moreno, F. J., Alonso-Blanco, E., Gerwig, H., Wiedensohler, A., Weinhold, K., Merkel, M., Bastian, S., Petit, J. E., Favez, O., Crumeyrolle, S., Ferlay, N., Martins Dos Santos, S., Putaud, J. P., Timonen, H., Lampilahti, J., Asbach, C., Wolf, C., Kaminski, H., Altug, H., Hoffmann, B., Rich, D. Q., Pandolfi, M., Harrison, R. M., Hopke, P. K., Petaja, T., Alastuey, A., and Querol, X.: Phenomenology of ultrafine particle concentrations and size distribution across urban Europe, Environ Int, 172, 107744, 10.1016/j.envint.2023.107744, 2023.

Varotsos, C., Ondov, J., Tzanis, C., Öztürk, F., Nelson, M., Ke, H., and Christodoulakis, J.: An observational study of the atmospheric ultra-fine particle dynamics, Atmospheric Environment, 59, 312-319, 10.1016/j.atmosenv.2012.05.015, 2012.

Wang, C., Xiang, J., Austin, E., Larson, T., and Seto, E.: Quantifying the contributions of road and air traffic to ambient ultrafine particles in two urban communities, Environ Pollut, 348, 123892, 10.1016/j.envpol.2024.123892, 2024.

Wang, Y. Q.: An Open Source Software Suite for Multi-Dimensional Meteorological Data Computation and Visualisation, Journal of Open Research Software, 7, 10.5334/jors.267, 2019.

Xiang, S., Zhang, S., Yu, Y. T., Wang, H., Deng, Y., Tan, Q., Zhou, Z., and Wu, Y.: Evaluating Ultrafine Particles and PM2.5 in Microenvironments with Health Perspectives: Variability in Concentrations and Pollutant Interrelationships, Aerosol and Air Quality Research, 23, 10.4209/aaqr.230046, 2023.

Zhang, R., Wang, G., Guo, S., Zamora, M. L., Ying, Q., Lin, Y., Wang, W., Hu, M., and Wang, Y.: Formation of urban fine particulate matter, Chem Rev, 115, 3803-3855, 10.1021/acs.chemrev.5b00067, 2015.

https://doi.org/10.5194/egusphere-2026-2195
Preprint. Discussion started: 19 May 2026

913 Zhao, S., Yu, Y., Li, J., Yin, D., Qi, S., and Qin, D.: Response of particle number concentrations to the clean air
914 action plan: lessons from the first long-term aerosol measurements in a typical urban valley in western China,
915 Atmospheric Chemistry and Physics, 21, 14959-14981, 10.5194/acp-21-14959-2021, 2021.

916